

Refined areal inequalities in gravitational field
(重力場中における精査された面積不等式)

LEE Kangjae
李 康載

Graduate School of Mathematics, Nagoya University
名古屋大学大学院 多元数理科学研究科

Contents

1	Introduction	2
1.1	Background: indicators for strong/weak gravity	2
1.2	Summary of main consequences	3
1.2.1	Definitions of four types of AGPSs	3
1.2.2	Refined areal inequality theorems	4
1.2.3	Organization and notation	5
2	General relativity and some basics	7
2.1	General relativity	7
2.2	Black hole	8
2.2.1	Schwarzschild black hole	8
2.2.2	Kerr black hole	10
2.3	Penrose inequality	11
2.3.1	Trapped surface	11
2.3.2	Geroch energy and inverse mean curvature flow	12
2.3.3	Proof of Penrose inequality by Jang and Wald	14
2.4	Komar angular momentum	15
2.5	Generalization of photon sphere	16
2.5.1	Photon surface	16
2.5.2	Dynamically transversely trapping surface	16
2.5.3	Loosely trapped surface	18
2.6	Attractive gravity probe surface	19
3	Refined areal inequalities for four-types of attractive gravity probe surfaces	20
3.1	Preliminaries	20
3.1.1	Some key formula	20
3.1.2	Some radii in axisymmetric spacetimes	23
3.2	Longitudinal attractive gravity probe surface	25
3.2.1	LAGPS associated with mean curvature (LAGPS-k)	25
3.2.2	LAGPS associated with Ricci scalar (LAGPS-r)	29
3.3	Transverse attractive gravity probe surface	31
3.3.1	TAGPS associated with mean curvature (TAGPS-k)	31
3.3.2	TAGPS associated with Ricci scalar (TAGPS-r)	34
4	Summary and outlook	37
A	Some geometric identities	38

Chapter 1

Introduction

1.1 Background: indicators for strong/weak gravity

Gravity is described by warped spacetime in general relativity. If gravity becomes strong, the orbit of light is curved. As a drastic case, general relativity predicts the existence of black hole so that even light cannot escape from it.

Trapped surface was introduced as an indicator for strong gravity region [1]. Under certain assumptions, the existence of the trapped surface shows us that spacetime is geodesically incomplete (singularity theorem [1, 2, 3]). However, if a singularity is hidden behind the event horizon which is the boundary of black hole, it is well-known that the trapped surface is also inside the black hole horizon [4]. Therefore, we cannot examine the singularity theorem from observational point of views.

Related to the above problem, we consider observable indicators for strong gravity region. In the Schwarzschild black hole which is the spherically symmetric solution to the vacuum Einstein equation, an unstable circular photon orbit exists outside the black hole. By virtue of the spherical symmetry, the set of these orbits forms a sphere, which is called the photon sphere. Recently other observable indicators for strong gravity region have been proposed as generalizations of the photon sphere to a wider class of spacetimes regardless of spherical symmetry, for examples, photon surface [5], loosely trapped surface (LTS) [6] and dynamically transversely trapping surface (DTTS) [7]. The LTS is defined by characterizing the strong curvature of space using the geometric quantity of mean curvature. In contrast, the DTTS is defined through the behavior of null geodesic congruences emitted along a timelike tube hypersurface, employing distinct geometric quantities for its characterization. Furthermore, the attractive gravity probe surface (AGPS) was introduced as an extension of the LTS to describe not only regions of strong gravity but also weak gravity regions [8]. This is achieved by looking at the behavior of the mean curvature in both regions.

Here note that, the Penrose inequality was proposed as the areal inequality for the trapped surface and that inequality is written by

$$A \leq 4\pi(2m)^2, \quad (1.1)$$

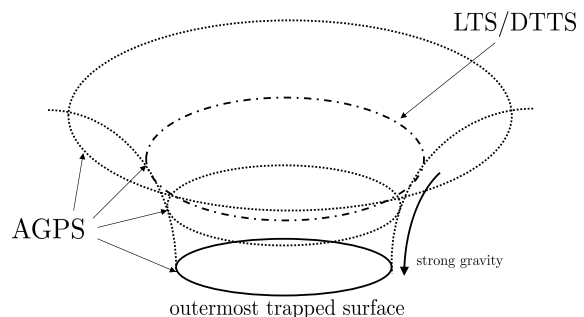


Figure 1.1: An image of the outermost trapped surface, LTS, DTTS, and AGPS. The AGPS encompasses the outermost trapped surface and LTS, and it exists even in weak gravity regions, such as near spatial infinity.

where A is the area of the outermost trapped surface, m is the mass of black hole [9]. It has been proven under certain assumptions on the time slices [10, 11, 12]. Furthermore, the Penrose inequality can be refined by taking account of contribution from angular momentum J as

$$A \leq 8\pi m \left(m + \sqrt{m^2 - J^2/m^2} \right). \quad (1.2)$$

Indeed, Anglada examined the above inequality for axisymmetric cases, and proved the refined Penrose-like inequality with the angular momentum and size for the minimal surface [13].

It is also natural to discuss the areal inequalities for LTS, DTTS, and AGPS [6, 7, 8], in a manner akin to the Penrose inequality. The authors of Refs. [6] and [7] proved that the area of the LTS and DTTS satisfies

$$A_{\text{LTS/DTTS}} \leq 4\pi(3m)^2. \quad (1.3)$$

For the AGPS, the areal inequality

$$A_{\text{AGPS}} \leq 4\pi \left[\frac{(3 + 4\alpha)m}{1 + 2\alpha} \right]^2 \quad (1.4)$$

also holds, where $\alpha > -1/2$ is an intensity parameter of gravity appeared in the definition of the AGPS later [8]. Eq. (1.4) reduces to Eq. (1.1) and Eq. (1.3) for the limits $\alpha \rightarrow \infty$ and $\alpha = 0$, respectively. The weak gravity region corresponds to the case where $0 > \alpha > -1/2$.

1.2 Summary of main consequences

In this thesis, we will present the following points based on my original works [14, 15].

- (i) A new extension of the DTTS to characterize weak gravity regions, which we refer to as transverse AGPS.
- (ii) Refined areal inequalities that take into account not only the angular momentum but also gravitational waves and matters.

1.2.1 Definitions of four types of AGPSs

The original version of AGPS is defined such that the first derivative of the mean curvature is controlled by the square of the mean curvature, multiplied by a certain factor (See Eq. (1.5)). However, we realized that a similar approach can be applied using the Ricci scalar of the surface (See Eq. (1.6)). Consequently, four types of AGPSs, extended from LTS and DTTS, can be introduced (See Table 1.1): the original AGPS (longitudinal AGPS associated with mean curvature, LAGPS-k), longitudinal AGPS associated with Ricci scalar (LAGPS-r), transverse AGPS associated with mean curvature (TAGPS-k), and transverse AGPS associated with Ricci scalar (TAGPS-r). The details are as follows (See also Definitions 3.8, 3.13, 3.17 and 3.20).

	Longitudinal AGPS (Extension of LTS)	Transverse AGPS (Extension of DTTS)
AGPS associated with mean curvature	original AGPS (LAGPS-k)	TAGPS-k
AGPS associated with Ricci scalar	LAGPS-r	TAGPS-r

Table 1.1: Four types of AGPSs

(a) Definition of longitudinal AGPS associated with mean curvature (LAGPS-k) (Izumi et al. [8], Lee et al. [14, 15]). An LAGPS-k, σ , is defined by a compact two-surface satisfying $k > 0$ on a spacelike hypersurface Σ and

$${}^{(3)}\mathcal{L}_r k \geq \alpha k^2, \quad (1.5)$$

where $\alpha > -1/2$ is a constant, k is the mean curvature of σ and ${}^{(3)}\mathcal{L}_r$ is Lie derivative on Σ with respect to the outward normal vector to σ .

(b) Definition of longitudinal AGPS associated with Ricci scalar (LAGPS-r) (Lee et al. [15]). An LAGPS-r, σ , is defined by a compact two-surface satisfying $k > 0$ on a spacelike hypersurface Σ and

$${}^{(3)}\mathcal{L}_r k \geq -{}^{(2)}R(1 - \gamma_L), \quad (1.6)$$

where γ_L is a constant, k is the mean curvature of σ and ${}^{(2)}R$ is the Ricci scalar of σ .

(c) Definition of transverse AGPS associated with mean curvature (TAGPS-k) (Lee et al [15]). A TAGPS-k, σ , is defined by a compact two-surface which is the intersection of the spacelike hypersurface Σ and timelike hypersurface S and satisfies the three conditions:

$$\kappa = 0, \quad (1.7)$$

$$\max(\bar{K}_{ab} k^a k^b) \leq -\beta k, \quad (1.8)$$

$${}^{(3)}\bar{\mathcal{L}}_n \kappa \leq 0, \quad (1.9)$$

where $\beta > -1/2$ is a constant, k is the mean curvature of σ , \bar{K}_{ab} is the extrinsic curvature of S , ${}^{(3)}\bar{\mathcal{L}}_n$ is the Lie derivative on S with respect to the unit normal vector to Σ , κ is the trace of the extrinsic curvature $\kappa_{ab} := (1/2){}^{(3)}\bar{\mathcal{L}}_n h_{ab}$ with the induced metric of σ , h_{ab} , k^a is an arbitrary null tangent vector to S with certain restriction about normalization (See Definition 3.17 for the detail) and the time lapse function is taken to be constant on σ .

(d) Definition of transverse AGPS associated with Ricci scalar (TAGPS-r) (Lee et al. [15]). In the same setup as those in the definition of TAGPS-k, a TAGPS-r, σ , is defined by a compact two-surface which satisfies the three conditions:

$$\kappa = 0, \quad (1.10)$$

$$\max(\bar{K}_{ab} k^a k^b) = 0, \quad (1.11)$$

$${}^{(3)}\bar{\mathcal{L}}_n \kappa \leq {}^{(2)}R(1 - \gamma_T), \quad (1.12)$$

where γ_T is a constant and ${}^{(2)}R$ is the Ricci scalar of σ .

1.2.2 Refined areal inequality theorems

For these surfaces, we could show the areal inequalities taking account of the angular momentum, gravitational waves and matters. See also Theorems 3.9, 3.14, 3.18 and 3.21 for the details.

(a) Refined areal inequality theorem for LAGPS-k (Lee et al. [14, 15]). *We assume that a four-dimensional spacetime satisfies the Einstein equation and Σ is an asymptotically flat spacelike maximal hypersurface equipped with the inverse mean curvature flow¹ $\{\sigma_y\}_{y \in \mathbb{R}}$. We*

¹The definition of the inverse mean curvature flow will be given in Subsec. 2.3.2.

suppose that each leaf σ_y is homeomorphic to a two-surface and the energy density of matters is non-negative. Then, we have an inequality for the LAGPS- k σ_0 ,

$$\begin{aligned} m_{\text{ADM}} - \left(m_{\text{ext}} + \frac{3}{3+4\alpha} m_{\text{int}} \right) &\geq \frac{1+2\alpha}{3+4\alpha} \mathcal{R}_{A0} + \frac{1}{\mathcal{R}_{A0}^3} \left(\bar{J}_{\min}^2 + \frac{3}{3+4\alpha} \bar{J}_0^2 \right) \\ &\geq \frac{1+2\alpha}{3+4\alpha} \mathcal{R}_{A0} + 2 \frac{3+2\alpha}{3+4\alpha} \frac{\bar{J}_{\min}^2}{\mathcal{R}_{A0}^3}, \end{aligned} \quad (1.13)$$

where m_{ADM} is the ADM mass, $\mathcal{R}_A(y)$ is the areal radius defined by $\mathcal{R}_A(y) := \sqrt{A(y)}/4\pi$, $\mathcal{R}_{A0} = \mathcal{R}_A(0)$, m_{ext} and m_{int} are regarded as the energy in the exterior and interior region of the LAGPS- k , respectively (See Eqs. (3.14) and (3.41)), \bar{J} is the area-averaged angular momentum of σ_0 (See Definition 3.4) and \bar{J}_{\min} is the minimum of the area-averaged angular momentum along σ_y .

(b) Refined areal inequality theorem for LAGPS-r (Lee et al. [15]). *In the same setup and under the same assumptions as those in the refined areal inequality theorem for LAGPS- k , we have an inequality for LAGPS-r σ_0 ,*

$$\begin{aligned} m_{\text{ADM}} - (m_{\text{int}} + m_{\text{ext}}) &\geq \frac{\gamma_L}{3} \mathcal{R}_{A0} + \frac{\bar{J}_0^2 + \bar{J}_{\min}^2}{\mathcal{R}_{A0}^3} \\ &\geq \frac{\gamma_L}{3} \mathcal{R}_{A0} + 2 \frac{\bar{J}_{\min}^2}{\mathcal{R}_{A0}^3}. \end{aligned} \quad (1.14)$$

(c) Refined areal inequality theorem for TAGPS-k (Lee et al. [15]). *In the same setup and under the same assumption as those in the refined areal inequality theorem for LAGPS- k , we have an inequality for TAGPS- k σ_0 , which possesses non-negative mean curvature,*

$$\begin{aligned} m_{\text{ADM}} + \frac{3}{3+4\beta} p_r^{(\text{int})} - m_{\text{ext}} &\geq \frac{1+2\beta}{3+4\beta} \mathcal{R}_{A0} + \frac{1}{\mathcal{R}_{A0}^3} \left(\frac{3}{3+4\beta} \bar{J}_0^2 + \bar{J}_{\min}^2 \right) \\ &\geq \frac{1+2\beta}{3+4\beta} \mathcal{R}_{A0} + 2 \frac{3+2\beta}{3+4\beta} \frac{\bar{J}_{\min}^2}{\mathcal{R}_{A0}^3}, \end{aligned} \quad (1.15)$$

where $p_r^{(\text{int})}$ is regarded as the radial pressure in the interior region of σ_0 (See Eq. (3.91)).

(d) Refined areal inequality theorem for TAGPS-r (Lee et al. [15]). *In the same setup and under the same assumption as those in the refined areal inequality theorem for LAGPS- k , we have an inequality for TAGPS-r σ_0 , which possesses non-negative mean curvature,*

$$\begin{aligned} m_{\text{ADM}} + p_r^{(\text{int})} - m_{\text{ext}} &\geq \frac{\gamma_T}{3} \mathcal{R}_{A0} + \frac{\bar{J}_0^2 + \bar{J}_{\min}^2}{\mathcal{R}_{A0}^3} \\ &\geq \frac{\gamma_T}{3} \mathcal{R}_{A0} + 2 \frac{\bar{J}_{\min}^2}{\mathcal{R}_{A0}^3}. \end{aligned} \quad (1.16)$$

As a specific example, we also consider areal inequalities for AGPSs in axisymmetric vacuum cases, incorporating the Komar angular momentum. See also Theorems 3.11, 3.15, 3.19 and 3.22 for the details.

1.2.3 Organization and notation

The rest of this thesis is organized as follows. In Chap. 2, we introduce general relativity. We also review the Penrose inequality with the proof by Jang and Wald [10]. In addition, we

shall give the review for the LTS, DTTS and AGPS. In Chap. 3, we provide the definition of new AGPSs and areal inequalities of four-types of AGPSs. In the first section, we prepare the setup and some key formulas for the proofs of the areal inequalities of AGPSs. Then, the next two sections present the areal inequalities of AGPSs with proofs. Note that Chap. 3 is based on my original work [14, 15]. The last chapter summarizes the entire thesis.

Throughout the thesis, we use the unit that the speed of light c and the gravitational constant G are $c = G = 1$. We use the abstract index notation by Wald as follows [3]. The vector is denoted by v^a with a latin index where it represents the vector itself, not its component. In the same way, the dual vector is also denoted by w_a . Therefore, the (k, l) -type tensor is expressed in $T^{a_1 \dots a_k}_{b_1 \dots b_l}$. We use the Einstein notation that we take the sum over the repeated index. We also use the notation ∂_μ instead of $\partial/\partial x^\mu$.

Acknowledgments

I am very grateful to my supervisor, T. Shiromizu for his invaluable support and encouragement. I am also grateful to co-researchers and professors including K. Izumi, H. Yoshino, Y. Tomikawa, H. Kanno and T. Nagao for their advice. I thank my family and friends including T. Kanai.

Chapter 2

General relativity and some basics

In this chapter, we provide a brief review of general relativity, covering topics such as the trapped surface, the Penrose inequality, and recent developments associated with these concepts, particularly those motivated by observations of black holes.

In Sec. 2.1, we present the fundamentals of Lorentzian geometry. Then, in Sec. 2.2, we introduce the Schwarzschild black hole solutions to the Einstein equation. We also see the event horizon and photon sphere which is composed of the circular orbit of photons. Next, in Sec. 2.3, we review the Penrose inequality [9] and its proof following Ref. [10]. In Sec. 2.4, we give the definition of the Komar angular momentum for axisymmetric spacetime [16] because we will focus on vacuum and axisymmetric cases in a part of the next chapter. We also present the result by Anglada, which provides a refined version of the Penrose-like inequality involving the Komar angular momentum [13]. In Sec. 2.5, we introduce the generalization of photon sphere, that is, the photon surface [5], LTS [6] and DTTS [7]. We provide the areal inequalities for LTS and DTTS without the proofs because they are included in the proofs for our new areal inequalities given in the next chapter. In Sec. 2.6, we also consider the AGPS [8] which is the generalization of the LTS so that it covers weak gravity region too.

2.1 General relativity

General relativity is a theory for four-dimensional spacetimes described by the Riemann geometry (M, g_{ab}) with the Lorentzian metric g_{ab} which has the sign of $(-, +, +, +)$. The covariant derivative ∇_a is determined by the Levi-Civita connection, such that $\nabla_c g_{ab} = 0$ and we also require the torsionless, which satisfies $\nabla_a \nabla_b \psi = \nabla_b \nabla_a \psi$ for scalar ψ in M . The Riemann curvature tensor $R_{abc}{}^d$ is defined as

$$R_{abc}{}^d v_d := (\nabla_a \nabla_b - \nabla_b \nabla_a) v_c, \quad (2.1)$$

where v^a is the vector in M . It is supposed that, the metric g_{ab} satisfies the Einstein equation

$$G_{ab} := R_{ab} - \frac{1}{2} R g_{ab} = 8\pi T_{ab}, \quad (2.2)$$

where $R_{ab} := R_{acb}{}^c$ is the Ricci tensor, $R := R_a{}^a$ is the scalar curvature, and T_{ab} is the energy-momentum tensor, which is zero if we consider the vacuum case.

In Lorentzian geometry, the vector v^a is classified by the three types, that is, timelike, null and spacelike depending on the following conditions for the norm,

$$g_{ab} v^a v^b < 0, \quad (2.3)$$

$$g_{ab} v^a v^b = 0, \quad (2.4)$$

$$g_{ab} v^a v^b > 0, \quad (2.5)$$

respectively. The hypersurface can also be characterized by its normal vector, where a timelike, null, or spacelike hypersurface corresponds to a spacelike, null, or timelike normal vector, respectively.

For every point p in the manifold M , we consider the null cone, which is the null hypersurface that passes through p at the origin of the tangent space. We assume that at each point p , the null cone is divided into two halves, known as the future half and the past half. These halves can be distinguished along every continuous curve in M . Accordingly, a future-directed vector is defined as one that lies within the future half of the null cone.

2.2 Black hole

In 1916, Schwarzschild discovered a significant exact solution to the Einstein equation [17]. Initially, it is thought that this solution was singular. However, its true structure was clarified by Kruskal in 1960 and then we know that the Schwarzschild spacetime describes the black hole [18]. Moreover, in the Schwarzschild spacetime, due to the strong gravity, there is the unstable circular orbit of photons outside the black hole. In Subsec 2.2.1, we look at the detail of the Schwarzschild spacetime. In another development, the Kerr solution, which describes a rotating vacuum black hole, was discovered in 1963 [19]. This solution will be presented in Subsec. 2.2.2.

2.2.1 Schwarzschild black hole

The Schwarzschild spacetime is the static and spherically symmetric solution to the vacuum Einstein equation, namely $G_{ab} = 0$. It is known that the Schwarzschild solution is the only spherically symmetric solution to the vacuum Einstein equations [20]. Remarkably, it has also been proven that the static vacuum black hole is unique to be the Schwarzschild solution [21].

The metric of the Schwarzschild solution is given by

$$ds^2 = -f(r)dt^2 + f^{-1}(r)dr^2 + r^2(d\theta^2 + \sin^2\theta d\phi^2), \quad (2.6)$$

where

$$f(r) = 1 - \frac{2m}{r} \quad (2.7)$$

and m is a constant which is the black hole mass.

The (t, t) and (r, r) -components of Eq. (2.6) become singular at $r = 0$ and $r = r_{\text{Sch}} := 2m$. The Kretschmann scalar $R_{abcd}R^{abcd} = 12r_{\text{Sch}}^2/r^6$ diverges at $r = 0$, so that we call $r = 0$ (curvature) singularity. On the other hand, the Kretschmann scalar is finite at $r = r_{\text{Sch}}$.

To analyze the $r = r_{\text{Sch}}$ surface, we consider the null geodesic along the radial direction in the Schwarzschild spacetime. So, we have

$$\frac{dt}{dr} = \pm \frac{1}{f(r)} \quad (2.8)$$

and then

$$t = \pm \int \frac{1}{f(r)} dr = \pm r^*, \quad (2.9)$$

where $r^* = r + r_{\text{Sch}} \log(r/r_{\text{Sch}} - 1)$. Using the new coordinate v and u defined by

$$v = t + r^*, \quad (2.10)$$

$$u = t - r^*, \quad (2.11)$$

the metric is rewritten as

$$ds^2 = - \left(1 - \frac{r_{\text{Sch}}}{r}\right) dvdu + r^2(d\theta^2 + \sin^2 \theta d\phi^2), \quad (2.12)$$

where r is related to u and v as $(v - u)/2 = r + r_{\text{Sch}} \log(r/r_{\text{Sch}} - 1)$. Finally, introducing the Kruskal coordinate (T, R) defined by

$$T = \frac{V + U}{2}, \quad R = \frac{V - U}{2}, \quad (2.13)$$

where $V = e^{v/2r_{\text{Sch}}}$ and $U = -e^{-u/2r_{\text{Sch}}}$, we rewrite the metric (2.12) as

$$ds^2 = \frac{4r_{\text{Sch}}^3 e^{-r/r_{\text{Sch}}}}{r} (-dT^2 + dR^2) + r^2(d\theta^2 + \sin^2 \theta d\phi^2). \quad (2.14)$$

From the definition of T and R , it is easy to see that

$$-T^2 + R^2 = (r/r_{\text{Sch}} - 1)e^{r/r_{\text{Sch}}}, \quad (2.15)$$

$$(T + R)/(R - T) = e^{t/r_{\text{Sch}}} \quad (2.16)$$

hold. Note that the metric (2.14) is nonsingular at $r = r_{\text{Sch}}$ as expected from the behavior of the Kretschmann invariant.

Now we draw the diagram by using the coordinates (T, R) (See Fig. 2.1). $r = 0$ and $r = r_{\text{Sch}}$ correspond to $-T^2 + R^2 = -1$ and $R = \pm T$, respectively. The radial null geodesics are represented by the lines where $T + R$ and $T - R$ are constants. The region where $T > 0$ and $-1 < -T^2 + R^2 < 0$ is defined as the black hole region because every future-directed null geodesic originating from any point within this region goes to $-T^2 + R^2 = -1$. We refer to the boundary of this region, where r equals r_{Sch} , as the event horizon.

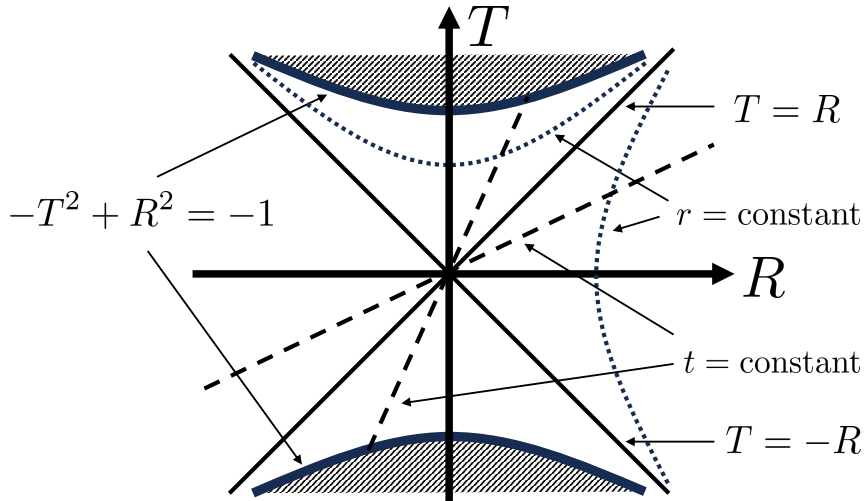


Figure 2.1: The Kruskal diagram in (T, R) .

Since the main topic of this thesis is the areal inequalities in gravitational fields, we look at the area of event horizon of the Schwarzschild black hole

$$A_{\text{Sch}} = 4\pi(2m)^2. \quad (2.17)$$

As shown in Sec. 2.3, one will be able to see that this gives us the upper bound of the areal inequality for the outermost trapped surface.

Next we consider another strong gravity indicator outside black holes. We consider null geodesics with angular momentum in the Schwarzschild spacetime. For the null geodesic with the tangent vector k^a on the $\theta = \pi/2$ -plane, we have the following conserved quantities associated with the two Killing vectors $\xi^a = (\partial_t)^a$, $\phi^a = (\partial_\phi)^a$ as

$$k^a \xi_a = -f(r)\dot{t} =: -E, \quad (2.18)$$

$$k^a \phi_a = r^2 \dot{\phi} =: L, \quad (2.19)$$

where the dot denotes the derivative with respect to the affine parameter. Using these conserved quantities, we rewrite the null condition $k^a k_a = 0$ as

$$\dot{r}^2 + \frac{f(r)L^2}{r^2} = E^2. \quad (2.20)$$

Then, we can identify the effective potential for the radial motion as

$$V_{\text{eff}} := \frac{f(r)L^2}{r^2} = \frac{L^2}{r^2} \left(1 - \frac{2m}{r}\right). \quad (2.21)$$

Since

$$\partial_r V_{\text{eff}} = -\frac{2L^2}{r^3} \left(1 - \frac{3m}{r}\right), \quad (2.22)$$

it is easy to see that there are unstable circular orbits at $r = 3m$. By virtue of the spherical symmetry, the set of the unstable circular orbits has the shape of the sphere. We call this set the photon sphere.

From the above, we see that in the Schwarzschild spacetime, the black hole horizon and the photon sphere are located at $r = 2m$ and $r = 3m$, respectively. Then, the region $2m < r \leq 3m$ can be regarded as the strong gravity region. In Subsec. 2.5.3 and Sec. 2.6, inspired by the above region in the Schwarzschild black hole, we will characterize strong gravity region for general cases.

2.2.2 Kerr black hole

Since objects are rotating in general, it is natural to consider a rotating black hole. Surprisingly, one knows that, under certain conditions, the stationary vacuum black hole is unique to be the Kerr spacetime given the mass and angular momentum [22].

The metric of Kerr spacetime is [19, 23]

$$ds^2 = -\frac{\Delta}{\rho^2} \left(dt - \frac{J}{m} \sin^2 \theta d\phi\right)^2 + \frac{\rho^2}{\Delta} dr^2 + \rho^2 d\theta^2 + \frac{\sin^2 \theta}{\rho^2} \left[\frac{J}{m} dt - \left(r^2 + \frac{J^2}{m^2}\right) d\phi\right]^2, \quad (2.23)$$

where J is the angular momentum and

$$\Delta := r^2 - 2mr + J^2/m^2, \quad (2.24)$$

$$\rho^2 := r^2 + (J^2/m^2) \cos^2 \theta. \quad (2.25)$$

It is known that the event horizon is located at $r = r_{\text{Kerr}} := m + \sqrt{m^2 - J^2/m^2}$, which is one of the roots of $\Delta = 0$ for $m^2 \geq |J|$.

Note that the area of event horizon of the Kerr black hole is

$$A_{\text{Kerr}} = 8\pi m \left(m + \sqrt{m^2 - J^2/m^2}\right), \quad (2.26)$$

and this is the upper bound of the inequality (1.2).

2.3 Penrose inequality

It is known that, under certain assumptions, the trapped surface is behind the event horizon and the area of event horizon is monotonically increasing [4]. From the above theorems, Penrose inequality is proposed that if the black hole settles down to the stationary state, then the area of the outermost trapped surface will be smaller than that of the event horizon at the final state of the black hole [9]. Since the Schwarzschild black hole has the largest area among all stationary black holes with the same mass and angular momentum, one can guess that Eq. (1.1) holds if black hole is actually formed.

In this section, we give the proof for the Penrose inequality by Jang and Wald [10]. We will employ it for proving the Penrose-like inequality of AGPSs in the next chapter. In Subsec. 2.3.1, after giving the definition of the trapped surface, we present a feature on totally geodesic spacelike hypersurface. In Subsec. 2.3.2, we introduce the Geroch energy and the inverse mean curvature flow to show the Penrose inequality. Then, we present the proof of the Penrose inequality by Jang and Wald in Subsec. 2.3.3.

2.3.1 Trapped surface

A trapped surface is introduced to describe the strong gravity region [1]. Let Σ be a three-dimensional spacelike hypersurface with the induced metric q_{ab} in the four-dimensional spacetime M . On Σ , we consider the two-surface σ with the induced metric h_{ab} . In the above setup, the trapped surface is defined as follows.

Definition 2.1 (trapped surface [2, 3]). Let σ be a smooth compact two-surface in spacelike hypersurface Σ . σ is a trapped surface, if and only if the expansion $\theta := h^{ab}\nabla_a k_b$ at all points in σ is negative where k^a is both the ingoing¹ and outgoing future-directed null geodesics orthogonal to σ .

One can consider the null hypersurface generated by the null geodesic congruence emanating from σ . Then, the expansion θ is rewritten as $\theta = (1/2)h^{ab}\mathcal{L}_k h_{ab} = \mathcal{L}_k \log \sqrt{\det h_{ab}}$, where \mathcal{L} is the Lie derivative in (M, g_{ab}) . Therefore, θ describes the variation of the area of the null congruence per unit area along the null geodesic.

One of the interesting geometrical object is the outer boundary of region where trapped surfaces exist. We call this the outermost trapped surface and one can show that $\theta = 0$ holds on outermost trapped surface (See Theorem 12.2.5 in [3] and Proposition 9.2.9 in [2]). Interestingly, on a totally geodesic spacelike hypersurface², one can show that the mean curvature of the outermost trapped surface vanishes.

Proposition 2.2. *For the totally geodesic spacelike hypersurface, the outermost trapped surface σ has the zero mean curvature.*

Proof. Let n^a and r^a be the timelike and spacelike unit normal vector to σ , respectively, and they are mutually orthogonal. One may take the outgoing future-directed null geodesics orthogonal to σ , $k^a = (n^a + r^a)/\sqrt{2}$, the expansion is calculated as³

$$\theta = h^{ab}\nabla_a k_b = \frac{1}{\sqrt{2}}h^{ab}\nabla_a(r_b + n_b) = \frac{1}{\sqrt{2}}(k + h^{ab}K_{ab}), \quad (2.29)$$

¹Note that the ingoing future-directed null geodesics are not relevant for characterizing strong gravity. Therefore, they will not be used from now on.

²If every geodesic of Σ is also a geodesic on M , we call Σ totally geodesic spacelike hypersurface, where it is known that Σ satisfies if and only if the extrinsic curvature of Σ is zero.

³The extrinsic curvature of Σ and the extrinsic curvature of σ are defined as

$$K_{ab} := q_a^c q_b^d \nabla_c n_d \quad (2.27)$$

where k is the mean curvature, that is, $k := k_a^a$. Since $\theta = 0$ holds at the outermost trapped surface, one can see from Eq. (2.29) that $k = 0$ holds on the totally geodesic spacelike hypersurface. \square

2.3.2 Geroch energy and inverse mean curvature flow

In this subsection, we introduce the Geroch energy and the inverse mean curvature flow. The Geroch energy is defined as follows.

Definition 2.3 (Geroch energy [24]). Geroch energy is the functional of σ defined as

$$E := \frac{A^{1/2}}{64\pi^{3/2}} \int_{\sigma} ({}^{(2)}R - k^2) dA, \quad (2.30)$$

where ${}^{(2)}R$ is the Ricci scalar of σ and A is the area of σ .

If σ is a two-sphere at spatial infinity, we can see that the Geroch energy becomes the Arnowitt-Deser-Misner (ADM) mass defined in an asymptotically flat spacelike hypersurface as follows.

Definition 2.4 (Arnowitt-Deser-Misner (ADM) mass [25, 3]). Let Σ be an asymptotically flat spacelike hypersurface that there exists a coordinate system $\{x^i\}$ such that at large r , i.e. $r \rightarrow \infty$, the induced metric of Σ in this system behaves

$$q_{ij} = \delta_{ij} + O(1/r), \quad (2.31)$$

where $r := [\sum_i (x^i)^2]^{1/2}$. Then, the ADM mass is defined by

$$m_{\text{ADM}} := \frac{1}{16\pi} \lim_{r \rightarrow \infty} \int_{S_r} (\partial^i q_{ij} - \partial_j q_i^i) r^j dA, \quad (2.32)$$

where S_r is a two-sphere with radius r and r^i is outward unit normal vector.

At a large sphere, the mean curvature of two-surface is given by

$$k = \frac{2}{r} \left(1 - \frac{m_{\text{ADM}}}{r}\right) + O\left(\frac{1}{r^3}\right), \quad (2.33)$$

where m_{ADM} is the ADM mass. By using Eq. (2.33) and the Gauss-Bonnet theorem, we can compute the Geroch energy as

$$\lim_{r \rightarrow \infty} E(r) = \lim_{r \rightarrow \infty} \frac{r}{32\pi} \left[16\pi - 4\pi r^2 \left(\frac{2}{r} \left(1 - \frac{m_{\text{ADM}}}{r}\right) \right)^2 \right] = m_{\text{ADM}}, \quad (2.34)$$

where we used $A(r) = 4\pi r^2[1 + O(1/r)]$. Then, we could confirm that the Geroch energy coincides with the ADM mass at spatial infinity.

Interestingly, one can show the monotonicity of the Geroch energy under certain assumptions which plays the important role in the proof of the Penrose inequality. We consider

and

$$k_{ab} := h_a^c h_b^d \nabla_c r_d, \quad (2.28)$$

respectively, where n^a is the timelike unit normal vector to Σ and r^a is the spacelike unit normal vector to σ . For the totally geodesic hypersurface, $K_{ab} = 0$ holds.

three-dimensional spacelike hypersurface Σ with the metric q_{ab} where Σ is supposed to be foliated by the spacelike two-surface $\{\sigma_y\}_{y \in \mathbb{R}}$ with the induced metric h_{ab} . The metric q_{ab} is decomposed as

$$q_{ab} = h_{ab} + r_a r_b, \quad (2.35)$$

where r^a is the spacelike unit normal vector of σ_y , and there is a radial lapse function φ so that one can write r_a as $r_a = \varphi(dy)_a$. For $\{\sigma_y\}_{y \in \mathbb{R}}$, we take the inverse mean curvature flow (IMCF) specified by the condition $k\varphi = 1$. In addition, we suppose that each σ_y is homeomorphic to a two-sphere (See Fig. 2.2).

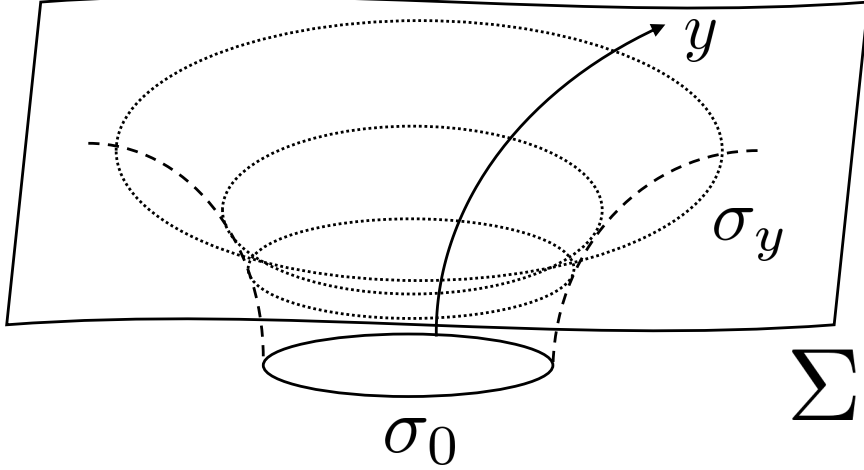


Figure 2.2: Spacelike hypersurface Σ is foliated with smooth inverse mean curvature flow (IMCF) $\{\sigma_y\}_{y \in \mathbb{R}}$ satisfying $k\varphi = 1$. The dotted two-surfaces stand for the each leaf σ_y .

It is easy to see that the IMCF exists in the spherically symmetric case. The induced metric of a spherically symmetric Σ can be written as

$$q_{ij}dx^i dx^j = g(r)dr^2 + r^2(d\theta^2 + \sin^2 \theta d\phi^2) = \varphi^2 dy^2 + r^2(y)(d\theta^2 + \sin^2 \theta d\phi^2), \quad (2.36)$$

where $g(r)$ is a function of r . The lapse function φ and the mean curvature of σ_y are given by

$$\varphi = g^{1/2} \frac{dr}{dy} \quad (2.37)$$

and

$$k = \frac{2}{r} \frac{1}{g^{1/2}}, \quad (2.38)$$

respectively. On the IMCF, the condition $k\varphi = 1$ implies

$$r(y) = r(0)e^{y/2}. \quad (2.39)$$

In general, on the IMCF, it is easy to see the following property for the area of σ_y .

Proposition 2.5 ([10]). *We assume that it is possible to take a smooth IMCF $\{\sigma_y\}_{y \in \mathbb{R}}$ on the spacelike hypersurface Σ . Then, for the area $A(y)$ of σ_y ,*

$$\frac{d}{dy} A(y) = A(y) \quad (2.40)$$

holds.

Proof. From the direct calculation,

$$\frac{d}{dy} A(y) = \frac{d}{dy} \int_{\sigma_y} dA = \int_{\sigma_y} k\varphi dA = \int_{\sigma_y} dA = A(y), \quad (2.41)$$

where we used $k\varphi = 1$ in the third equality. \square

By using the above proposition, we have the following proposition for the Geroch energy.

Proposition 2.6 ([24]). *We assume that it is possible to take a smooth IMCF $\{\sigma_y\}_{y \in \mathbb{R}}$ on the spacelike hypersurface Σ , where the each leaf σ_y is homeomorphic to a two-sphere. Then, we obtain*

$$\frac{dE}{dy} = \frac{A^{1/2}}{64\pi^{3/2}} \int_{\sigma_y} \left[2\varphi^{-2}(\mathcal{D}\varphi)^2 + {}^{(3)}R + \tilde{k}_{ab}\tilde{k}^{ab} \right] dA, \quad (2.42)$$

where ${}^{(3)}R$ is the Ricci scalar of Σ , \mathcal{D}_a is covariant derivative on σ_y and \tilde{k}_{ab} is the traceless part of the extrinsic curvature k_{ab} of σ_y , i.e. $\tilde{k}_{ab} = k_{ab} - (k/2)h_{ab}$ with the induced metric of σ_y , h_{ab} .

Proof. First we note that the Geroch energy becomes

$$E(y) = \frac{A^{1/2}(y)}{4\pi^{1/2}} - \frac{A^{1/2}(y)}{64\pi^{3/2}} \int_{\sigma_y} k^2 dA, \quad (2.43)$$

where we used the Gauss-Bonnet theorem for σ_y , that is, $\int_{\sigma_y} {}^{(2)}R dA = 8\pi$. By using Eq. (A.8) in Appendix A and the double trace for the Gauss equations on σ_y in Σ ,

$${}^{(2)}R = {}^{(3)}R - 2{}^{(3)}R_{ab}r^a r^b + k^2 - k_{ab}k^{ab}, \quad (2.44)$$

the derivative for the second term in the right-hand side of Eq. (2.43) with respect to y is computed as

$$\frac{d}{dy} \int_{\sigma_y} k^2 dA = - \int_{\sigma_y} \left(2\varphi^{-1} \mathcal{D}^2 \varphi + {}^{(3)}R + \tilde{k}_{ab}\tilde{k}^{ab} \right) dA + 8\pi - \frac{1}{2} \int_{\sigma_y} k^2 dA. \quad (2.45)$$

Then, Eqs. (2.43) and (2.45) with Proposition 2.5 imply Eq. (2.42). \square

If ${}^{(3)}R \geq 0$ holds, one can easily see the monotonicity of the Geroch energy.

Corollary 2.7. *In the same setup as those in Proposition 2.6, we assume that ${}^{(3)}R \geq 0$ holds on Σ . Then, the Geroch energy of σ_y is monotonically nondecreasing.*

2.3.3 Proof of Penrose inequality by Jang and Wald

If ${}^{(3)}R \geq 0$ on the spacelike hypersurface Σ , we have the following theorem from Corollary 2.7.

Theorem 2.8 ([10]). *Let Σ be an asymptotically flat totally geodesic spacelike hypersurface with non-negative scalar curvature ${}^{(3)}R \geq 0$, equipped with the inverse mean curvature flow $\{\sigma_y\}_{y \in \mathbb{R}}$ where σ_0 is an outermost trapped surface. We suppose that each leaf σ_y is homeomorphic to a two-sphere. Then, we have an inequality for the outermost trapped surface σ_0 ,*

$$m_{\text{ADM}} \geq \frac{\mathcal{R}_{A_0}}{2}, \quad (2.46)$$

where m_{ADM} is the ADM mass and $\mathcal{R}_{A_0} = \sqrt{A_0/4\pi}$ with the area of σ_0 , A_0 .

Proof. From Corollary 2.7, we see

$$\frac{dE}{dy} \geq 0. \quad (2.47)$$

The integral of the above inequality over y in the range $0 \leq y \leq \infty$ gives us

$$m_{\text{ADM}} \geq E(0). \quad (2.48)$$

With Proposition 2.2, Eq. (2.43) shows us $E(0) = \mathcal{R}_{A0}/2$ and then we see Eq. (2.46). \square

2.4 Komar angular momentum

For axisymmetric spacetimes, we can naturally consider the angular momentum for the two-surface associated with the axial Killing vector [16]. Here, we follow the setup of Subsec. 2.3.1.

Definition 2.9 (Komar angular momentum [16]). Using the axial Killing vector ϕ^a , one can define the Komar angular momentum J ,

$$J := \frac{1}{8\pi} \int_{\sigma} K_{ab} \phi^a r^b dA. \quad (2.49)$$

Note that if Σ is foliated by $\{\sigma_y\}_{y \in \mathbb{R}}$, $J(y)$ does not depend on y when the vacuum Einstein equation holds (See Ref. [13]), and hence, we simply denote J rather than $J(y)$ in the case of vacuum axisymmetric spacetimes. In the next chapter, we also use the Komar angular momentum to refine the areal inequalities for the AGPSs in that case.

With the Komar angular momentum, Anglada proved the refined Penrose-like inequality for the minimal surface in vacuum axisymmetric spacetimes as the following theorem. The proof of the theorem is omitted in this section, as it will be included in the proof presented in the next chapter.

Theorem 2.10 ([13]). *Let M be an axisymmetric spacetime satisfying the vacuum Einstein equation (2.2), and Σ be an asymptotically flat axisymmetric spacelike maximal hypersurface equipped with the inverse mean curvature flow $\{\sigma_y\}_{y \in \mathbb{R}}$ where σ_0 is an compact and connected minimal surface. We suppose that Σ has no other trapped surface and each leaf σ_y is homeomorphic to a two-surface. Then, we have an inequality for the σ_0 ,*

$$m_{\text{ADM}} \geq \frac{\mathcal{R}_{A0}}{2} + \frac{J^2}{\mathcal{R}_0^2 \mathcal{R}_{A0}}, \quad (2.50)$$

where m_{ADM} is the ADM mass, J is the angular momentum, $\mathcal{R}_{A0} := \sqrt{A_0/4\pi}$ and $\mathcal{R}_0 = \mathcal{R}(0)$ is defined by

$$\frac{1}{\mathcal{R}^2} := 4\pi \mathcal{R}_A \int_y^\infty \frac{\mathcal{R}_A}{\int_{\sigma_{y'}} \phi_a \phi^a dA} dy'. \quad (2.51)$$

Multiplying Eq. (2.50) by $\mathcal{R}_{A0}/2$ with $m_{\text{ADM}} \geq \mathcal{R}_{A0}/2$ implies [13]

$$m_{\text{ADM}}^2 \geq \left(\frac{\mathcal{R}_{A0}}{2}\right)^2 + \frac{J^2}{2\mathcal{R}_0^2}. \quad (2.52)$$

We can see that the equality of Eq. (2.52) is similar to the following formula,

$$m^2 = \left(\frac{\mathcal{R}}{2}\right)^2 + \frac{J^2}{\mathcal{R}^2} = \frac{A}{16\pi} + 4\pi \frac{J^2}{A}, \quad (2.53)$$

where $\mathcal{R} := \sqrt{A/4\pi}$. In fact, the area of the event horizon for the Kerr black hole given by Eq. (2.26) satisfies Eq. (2.53), i.e. $A = A_{\text{Kerr}}$.

2.5 Generalization of photon sphere

In the Schwarzschild black hole spacetime, an unstable circular photon orbit (photon sphere) exists. In this section, we introduce the photon surface, DTTS and LTS as the generalizations of photon sphere. The Penrose-like inequalities for LTS and DTTS are presented in this section without proofs, as these will be included in the discussions of the refined Penrose-like inequality in the next chapter.

2.5.1 Photon surface

The photon sphere is an observable indicator of strong gravity, although it is defined only in spherically symmetric spacetimes. The photon surface was proposed as a natural generalization of the photon sphere to general cases:

Definition 2.11 (photon surface [5]). S is a photon surface if and only if it is a timelike hypersurface such that every null geodesic in M originating from any point $p \in S$ stays within S .

One can see that the photon surface has the following property.

Proposition 2.12 ([5]). *Let (S, p_{ab}) be the photon surface with the induced metric p_{ab} . Then, on all points on S for any null tangent vector of the geodesic k^a , we have*

$$\bar{K}_{ab}k^ak^b = 0, \quad (2.54)$$

where $\bar{K}_{ab} := p_a^cp_b^d\nabla_cr_d$ is the extrinsic curvature with a unit normal vector to S , r^a .

Proof. From the definition of the photon surface, on every point of S , there is a null geodesic in M such that k^a is the tangent vector so that, k^a satisfies $k^a\nabla_ak^b = 0$. Since k^a is also tangent to S , $r_ak^a = 0$ holds. Then, we see

$$\bar{K}_{ab}k^ak^b = k^ak^bp_a^cp_b^d\nabla_cr_d = k^a\nabla_ar_bk^b = k^a\nabla_a(r_bk^b) = 0, \quad (2.55)$$

where we used $k^ap_a^b = k^b$ in the second equality and $r_ak^a = 0$ in the last equality. \square

On the photon surface S , it is also shown that \bar{K}_{ab} is traceless [5]. This is relatively strong requirement for the geometry of S so that the photon surfaces do not exist in general. Moreover, photon surfaces exist even in the Minkowski spacetime, indicating that they do not necessarily represent regions of strong gravity. Then, it is nice to introduce another indicator for the strong gravity.

2.5.2 Dynamically transversely trapping surface

To consider an extension of the photon surface, we give the setup and notations. Let us consider a three-dimensional spacelike hypersurface (Σ, q_{ab}) and a three-dimensional timelike hypersurface (S, p_{ab}) in a four-dimensional spacetime (M, g_{ab}) . For our current purpose, we suppose that there is the intersection of a surface (σ_0, h_{ab}) between S and Σ , and Σ to be orthogonal to S (See Fig. 2.3). With the future-directed timelike unit normal vector n^a to Σ and the outward spacelike unit normal vector r^a to S , the metric g_{ab} is decomposed as

$$g_{ab} = q_{ab} - n_an_b = p_{ab} + r_ar_b = h_{ab} - n_an_b + r_ar_b. \quad (2.56)$$

Let φ be the lapse function with respect to r^a , i.e. $r_a = \varphi(dy)_a$ where the coordinate y is chosen so that a $y = \text{constant}$ hypersurface corresponds to S . N is the lapse function with respect to n^a , i.e. $n_a = -N(dt)_a$ where the coordinate t is chosen so that a $t = \text{constant}$ hypersurface corresponds to Σ . The extrinsic curvature of Σ and S are written by

$$K_{ab} = \frac{1}{2} \mathcal{L}_n q_{ab} \quad (2.57)$$

and

$$\bar{K}_{ab} = \frac{1}{2} \mathcal{L}_r p_{ab}, \quad (2.58)$$

respectively, where \mathcal{L} is the Lie derivative in (M, g_{ab}) . For (σ_0, h_{ab}) , one can define the two extrinsic curvatures as

$$k_{ab} = \frac{1}{2} {}^{(3)}\mathcal{L}_r h_{ab} \quad (2.59)$$

and

$$\kappa_{ab} = \frac{1}{2} {}^{(3)}\bar{\mathcal{L}}_n h_{ab}, \quad (2.60)$$

where ${}^{(3)}\mathcal{L}$ and ${}^{(3)}\bar{\mathcal{L}}$ are the Lie derivatives in Σ and S , respectively.

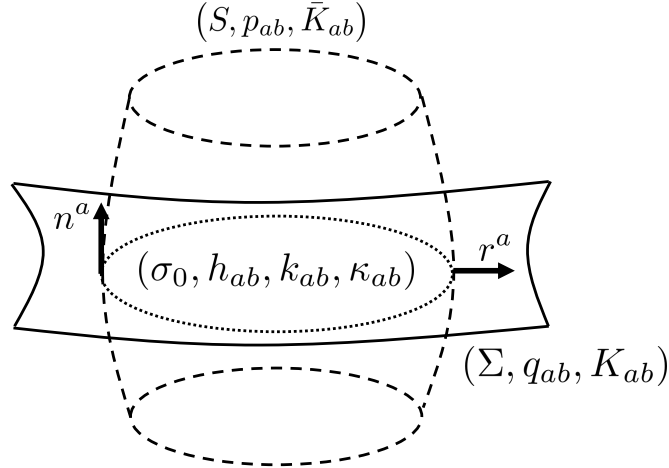


Figure 2.3: A picture of three-dimensional spacelike hypersurface Σ , three-dimensional timelike hypersurface S and the intersection σ_0 .

In the above setup, we define the dynamically transversely trapping surface (DTTS) as follows.

Definition 2.13 (dynamically transversely trapping surface [7]). A DTTS σ_0 is defined by a compact two-surface satisfying the following three conditions:

$$\kappa = 0, \quad (2.61)$$

$$\max(\bar{K}_{ab} k^a k^b) = 0, \quad (2.62)$$

$${}^{(3)}\bar{\mathcal{L}}_n \kappa \leq 0, \quad (2.63)$$

where $\kappa = h^{ab} \kappa_{ab}$, k^a is an arbitrary null tangent vector to S and the lapse function N is taken to be constant on σ_0 .

The conditions of Eqs. (2.61), (2.62) and (2.63) are called the momentarily non-expanding condition, the marginally transversely trapping condition, and the accelerated contraction condition, respectively.

We analyze the Schwarzschild spacetime to see the conditions of Eqs. (2.61), (2.62) and (2.63). For simplicity, we adopt Σ and S as the $t = \text{constant}$ and $r = \text{constant}$ hypersurfaces, respectively. In this case, $\kappa = 0$ holds everywhere, and then the conditions of Eqs. (2.61) and (2.63) are trivially satisfied, while the condition of Eq. (2.62) becomes non-trivial. Adopting $k^a = n^a + s^a$, where s^a is a spatial unit vector tangent to S and orthogonal to n^a , one can compute $\bar{K}_{ab}k^ak^b$ as

$$\bar{K}_{ab}k^ak^b = \bar{K}_{(n)} + \frac{1}{2}k = \frac{1}{r\sqrt{f}} \left(1 - \frac{3m}{r} \right), \quad (2.64)$$

where we used $\bar{K}_{(n)} := \bar{K}_{ab}n^an^b = -(1/2)f^{-1/2}\partial_r f$ and $k = 2f^{1/2}/r$. Therefore, the condition of Eq. (2.62) implies $r = 3m$, that is, the location of the photon sphere of the Schwarzschild spacetime.

In the last of this subsection, we show the Penrose-like inequality for the DTTS. We skip the proof because it will be included into that for Theorem 3.18 in Subsec. 3.3.1.

Theorem 2.14 ([7]). *Let Σ be an asymptotically flat spacelike totally geodesic hypersurface equipped with the inverse mean curvature flow $\{\sigma_y\}_{y \in \mathbb{R}}$ where σ_0 is a convex DTTS. We suppose that each leaf σ_y is homeomorphic to a two-surface. Then, if ${}^{(3)}R \geq 0$, $G_{ab}r^ar^b \leq 0$ on σ_0 and $k > 0$ at least at one point on σ_0 , we have an inequality for the DTTS σ_0 ,*

$$m_{\text{ADM}} \geq \frac{\mathcal{R}_{A0}}{3}, \quad (2.65)$$

where m_{ADM} is the ADM mass and $\mathcal{R}_{A0} = \sqrt{A_0/4\pi}$ with the area of σ_0 , A_0 .

2.5.3 Loosely trapped surface

In previous two subsections, the photon surface and DTTS were defined based on the behavior of the null geodesic. On the other hand, the loosely trapped surface (LTS) is defined by the mean curvature as follows.

Definition 2.15 (loosely trapped surface [6]). Let k be the mean curvature of σ_0 on the three-dimensional spacelike hypersurface Σ . An LTS σ_0 is defined by a compact two-surface satisfying $k > 0$ and

$${}^{(3)}\mathcal{L}_r k \geq 0. \quad (2.66)$$

Let us consider the Schwarzschild spacetime with the metric (2.6). For $r = \text{constant}$ surfaces in $t = \text{constant}$ hypersurfaces, the left-hand side of Eq. (2.66) is computed as

$${}^{(3)}\mathcal{L}_r k = -\frac{2}{r^2} \left(1 - \frac{3m}{r} \right). \quad (2.67)$$

The condition of Eq. (2.66) holds for $r \leq 3m$ and the equality gives us $r = 3m$, that is, the location of the photon sphere of the Schwarzschild spacetime.

In the similar way to the proof of Theorem 2.8 on the Penrose inequality, we can have the Penrose-like inequality for the LTS. We skip the proof because it will be included into that for Theorem 3.9 in Subsec. 3.2.1.

Theorem 2.16 ([6]). *Let Σ be an asymptotically flat spacelike hypersurface with non-negative scalar curvature ${}^{(3)}R \geq 0$, equipped with the inverse mean curvature flow $\{\sigma_y\}_{y \in \mathbb{R}}$ where σ_0 is an LTS. We suppose that each leaf σ_y is homeomorphic to a two-surface. Then, we have an inequality for the LTS σ_0 ,*

$$m_{\text{ADM}} \geq \frac{\mathcal{R}_{A0}}{3}, \quad (2.68)$$

where m_{ADM} is the ADM mass and $\mathcal{R}_{A0} = \sqrt{A_0/4\pi}$ with the area of σ_0 , A_0 .

2.6 Attractive gravity probe surface

Attractive gravity probe surface (AGPS) was proposed as an extension of the LTS to weak gravity region as well as strong one [8]. The definition is as follows.

Definition 2.17 (attractive gravity probe surface [8]). An attractive gravity probe surface (AGPS) is defined by a compact two-surface satisfying $k > 0$ on spacelike hypersurface Σ and

$${}^{(3)}\mathcal{L}_r k \geq \alpha k^2, \quad (2.69)$$

where α is a constant greater than $-1/2$.

Note that one can specify the strength of gravity by the intensity parameter α . We imposed $\alpha > -1/2$ because the situation satisfying $\alpha \leq -1/2$ would correspond to the case that the gravity is repulsive. An AGPS with α being close to minus one half exists near asymptotic infinity and thus it is likely that our inequality for an AGPS holds even for weak gravity.

As a simple example, let us consider the Schwarzschild spacetime. When we assume that m in the metric (2.6) is non-negative and $\alpha > -1/2$, the condition of Eq. (2.69) implies

$$r \leq \frac{3 + 4\alpha}{1 + 2\alpha} m. \quad (2.70)$$

For $\alpha \rightarrow -1/2$, the right-hand side diverges and the condition can be satisfied by a surface with an arbitrarily large r . We see that $r \leq 3m$ for $\alpha = 0$ and $r \leq 2m$ for the $\alpha \rightarrow \infty$ limit.

To discuss the meaning of Definition 2.17 further, it is nice to see more general static spherically symmetric spacetimes with the metric

$$ds^2 = -f_1(r)dt^2 + \frac{dr^2}{f_2(r)} + r^2(d\theta^2 + \sin^2\theta d\phi^2). \quad (2.71)$$

For this, the condition of Eq. (2.69) becomes

$${}^{(3)}\mathcal{L}_r k - \alpha k^2 = \frac{1}{r} \left[f_2' - \frac{2(1 + 2\alpha)}{r} f_2 \right] \geq 0. \quad (2.72)$$

Supposing the positivity of f_2 , we rewrite it as

$$f_2' \geq \frac{2(1 + 2\alpha)}{r} f_2 \geq 0. \quad (2.73)$$

Then, one can see that f_2 is a monotonically increasing function, which corresponds to the attractive property of gravity, as long as $\alpha > -1/2$ holds.

The monotonicity of the Geroch energy and IMCF gives us the Penrose-like inequality. We again skip the proof because it will be included into that for Theorem 3.9 in Subsec. 3.2.1.

Theorem 2.18 ([8]). *Let Σ be an asymptotically flat spacelike hypersurface with non-negative scalar curvature ${}^{(3)}R \geq 0$, equipped with the inverse mean curvature flow $\{\sigma_y\}_{y \in \mathbb{R}}$ where σ_0 is an AGPS. We suppose that each leaf σ_y is homeomorphic to a two-surface. Then, we have the inequality for the AGPS σ_0 ,*

$$m_{\text{ADM}} \geq \frac{1 + 2\alpha}{3 + 4\alpha} \mathcal{R}_{A_0}, \quad (2.74)$$

where m_{ADM} is the ADM mass and $\mathcal{R}_{A_0} = \sqrt{A_0/4\pi}$ with the area of σ_0 , A_0 .

Chapter 3

Refined areal inequalities for four-types of attractive gravity probe surfaces

In Subsecs. 2.5.2, 2.5.3 and Sec. 2.6, we presented generalizations and extensions of the photon sphere, including the DTTS, LTS, and AGPS [6, 7, 8]. Additionally, we discussed areal inequalities for these surfaces. However, these inequalities did not account for contributions from angular momentum, gravitational waves, and matters. Recently, Anglada proposed a refined Penrose-like inequality that incorporates angular momentum for minimal surfaces in axisymmetric spacetimes (Theorem 2.10) [13]. We also plan to extend DTTS to cover weak gravity regions and introduce a new method for characterizing gravity's intensity. This chapter introduces refined areal inequalities for four types of AGPSs: the original AGPS, an extension from LTS, and two from DTTS, without any imposed symmetry. We will also explore axisymmetric vacuum cases as a specific example. Sec. 3.1 reviews geometric formulas and re-examines the variation of Geroch energy with IMCF crucial for the main theorem in the final two sections. The concluding two sections focus on refining the Penrose-like inequalities for AGPSs. This chapter lies in my original works [14, 15].

3.1 Preliminaries

In the proof of the Penrose inequality by Jang and Wald, the monotonicity of the Geroch energy along IMCF played an important role (See Theorem 2.8). In this section, we refine the variation of Geroch energy with IMCF taking into account of the contribution from the angular momentum, gravitational waves and matters.

3.1.1 Some key formula

In this subsection, we consider the same setup as in Subsec. 2.5.2. For the convenience, we decompose the extrinsic curvature K_{ab} and \bar{K}_{ab} as

$$K_{ab} = K_{(r)}r_a r_b + \kappa_{ab} + v_a r_b + v_b r_a \quad (3.1)$$

and

$$\bar{K}_{ab} = \bar{K}_{(n)}n_a n_b + k_{ab} + v_a n_b + v_b n_a, \quad (3.2)$$

where $K_{(r)} := K_{ab}r^a r^b$, $\bar{K}_{(n)} := \bar{K}_{ab}n^a n^b$, and $v_a := h_{ab}r^c K_c^b = -h_{ab}n^c \bar{K}_c^b$. Then, from the definition of the Ricci tensor and by using the Gauss equation, we obtain the following two key identities as propositions.

Proposition 3.1 ([14, 15]). *In the same setup as those in Subsec. 2.5.2,*

$${}^{(3)}\mathfrak{L}_r k = \frac{1}{2}{}^{(2)}R - G_{ab}n^a n^b + \kappa K_{(r)} + \frac{1}{2}(\kappa^2 - \kappa_{ab}\kappa^{ab} - k^2 - k_{ab}k^{ab}) - v_a v^a - \varphi^{-1}\mathcal{D}^2\varphi \quad (3.3)$$

holds, where ${}^{(2)}R$ is the Ricci scalar of (σ_0, h_{ab}) , G_{ab} is the Einstein tensor for (M, g_{ab}) and \mathcal{D}_a is the covariant derivative with respect to (σ_0, h_{ab}) .

Proof. The Lie derivative of the trace of mean curvature k of σ_0 along the r^a -direction is calculated as (See Appendix A)

$${}^{(3)}\mathfrak{L}_r k = -{}^{(3)}R_{ab}r^a r^b - k_{ab}k^{ab} - \varphi^{-1}\mathcal{D}^2\varphi, \quad (3.4)$$

where ${}^{(3)}R_{ab}$ is the Ricci tensor of (Σ, q_{ab}) . With the double trace of the Gauss equations on σ_0 in Σ and Σ in M , we have

$${}^{(2)}R = {}^{(3)}R - 2{}^{(3)}R_{ab}r^a r^b + k^2 - k_{ab}k^{ab} \quad (3.5)$$

and

$${}^{(3)}R = 2G_{ab}n^a n^b - K^2 + K_{ab}K^{ab}, \quad (3.6)$$

where ${}^{(3)}R$ is Ricci scalar of (Σ, q_{ab}) . Then, with Eqs. (3.5) and (3.6), Eq. (3.4) becomes

$${}^{(3)}\mathfrak{L}_r k = \frac{1}{2}{}^{(2)}R - G_{ab}n^a n^b + \frac{1}{2}(K^2 - K_{ab}K^{ab} - k^2 - k_{ab}k^{ab}) - \varphi^{-1}\mathcal{D}^2\varphi, \quad (3.7)$$

and, using Eq. (3.1), we have Eq. (3.3). \square

Proposition 3.2 ([15]). *In the same setup as those in Proposition 3.1,*

$${}^{(3)}\bar{\mathfrak{L}}_n \kappa = -\frac{1}{2}{}^{(2)}R - G_{ab}r^a r^b - k\bar{K}_{(n)} + \frac{1}{2}(k^2 - k_{ab}k^{ab} - \kappa^2 - \kappa_{ab}\kappa^{ab}) + v_a v^a + N^{-1}\mathcal{D}^2 N. \quad (3.8)$$

Proof. Similarly to Eq. (3.4), the Lie derivative of κ along the n^a -direction is written as (See Appendix A)

$${}^{(3)}\bar{\mathfrak{L}}_n \kappa = -{}^{(3)}\bar{R}_{ab}n^a n^b - \kappa_{ab}\kappa^{ab} + N^{-1}\mathcal{D}^2 N, \quad (3.9)$$

where ${}^{(3)}\bar{R}_{ab}$ is the Ricci tensor of (S, p_{ab}) . Taking the double trace for the Gauss equations on σ_0 in S and S in M , we have

$${}^{(2)}R = {}^{(3)}\bar{R} + 2{}^{(3)}\bar{R}_{ab}n^a n^b - \kappa^2 + \kappa_{ab}\kappa^{ab} \quad (3.10)$$

and

$${}^{(3)}\bar{R} = -2G_{ab}r^a r^b + \bar{K}^2 - \bar{K}_{ab}\bar{K}^{ab}, \quad (3.11)$$

where ${}^{(3)}\bar{R}$ is Ricci scalar of (S, p_{ab}) . Then, with Eqs. (3.10) and (3.11), Eq. (3.9) is rewritten as

$${}^{(3)}\bar{\mathfrak{L}}_n \kappa = -\frac{1}{2}{}^{(2)}R - G_{ab}r^a r^b + \frac{1}{2}(\bar{K}^2 - \bar{K}_{ab}\bar{K}^{ab} - \kappa^2 - \kappa_{ab}\kappa^{ab}) + N^{-1}\mathcal{D}^2 N, \quad (3.12)$$

and, using (3.2), we obtain Eq. (3.8). \square

Note that we have not used the Einstein equation up to now, and the above equations are geometric identities.

In this section, by taking account of contribution from angular momentum, gravitational waves and matters, we give the derivation for the key formula obtained through the monotonicity of Geroch energy on the hypersurface equipped with the inverse mean curvature flow (IMCF). The integration of Eq. (2.42) over y in the range $0 \leq y < \infty$ leads us to the key formula of this thesis.

Lemma 3.3 ([14]). *We assume that spacetime M satisfies the Einstein equation (2.2) and Σ is an asymptotically flat spacelike maximal hypersurface equipped with the inverse mean curvature flow $\{\sigma_y\}_{y \in \mathbb{R}}$. We suppose that each leaf σ_y is homeomorphic to a two-surface. If $\rho := T_{ab}n^a n^b \geq 0$ holds where n^a is the future-directed unit normal vector to Σ , the following inequality holds*

$$m_{\text{ADM}} - m_{\text{ext}} - \frac{\mathcal{R}_{A0}}{2} + \frac{\mathcal{R}_{A0}}{32\pi} \int_{\sigma_0} dA k^2 \geq \frac{1}{16\pi} \int_0^\infty dy \mathcal{R}_A(y) \int_{\sigma_y} dA v^a v_a, \quad (3.13)$$

where m_{ADM} is the ADM mass, $\mathcal{R}_A(y)$ is the areal radius defined by $\mathcal{R}_A(y) := \sqrt{A(y)/4\pi}$ and $\mathcal{R}_{A0} = \mathcal{R}_A(0)$. And m_{ext} is defined as

$$m_{\text{ext}} := 2\pi \int_0^\infty dy \mathcal{R}_A^3(y) \bar{\rho}_{\text{tot}}(y), \quad (3.14)$$

where $\bar{\rho}_{\text{tot}}$ is the surface-averaged one for the total energy density $\rho_{\text{tot}} := \rho + \rho_{\text{gw}}$,

$$\bar{\rho}_{\text{tot}}(y) := \frac{1}{A} \int_{\sigma_y} dA \rho_{\text{tot}} \quad (3.15)$$

and

$$8\pi \rho_{\text{gw}} := \frac{1}{2} (\tilde{\kappa}_{ab} \tilde{\kappa}^{ab} + \tilde{k}_{ab} \tilde{k}^{ab}), \quad (3.16)$$

where $\tilde{\kappa}_{ab}$ and \tilde{k}_{ab} are the traceless part of κ_{ab} and k_{ab} , respectively.

Proof. Using Eqs. (3.6) and (3.1) with the Hamiltonian constraint of the Einstein equations, $G_{ab}n^a n^b = 8\pi T_{ab}n^a n^b$, we rewrite the three-dimensional Ricci scalar ${}^{(3)}R$ of Σ as

$${}^{(3)}R = 16\pi\rho + 2v_a v^a + \tilde{\kappa}_{ab} \tilde{\kappa}^{ab} - 2\kappa K_{(r)} - \frac{1}{2}\kappa^2. \quad (3.17)$$

Using Eq. (3.17) with the maximal slice condition (i.e., $K = K_{(r)} + \kappa = 0$) and the positivity of energy density for matters, $\rho \geq 0$, then, from Eq. (2.42), we find

$$\frac{dE}{dy} = \frac{A^{1/2}}{64\pi^{3/2}} \int_{\sigma_y} \left[2\varphi^{-2} (\mathcal{D}\varphi)^2 + 16\pi\rho_{\text{tot}} + 2v_a v^a + \frac{3}{2}\kappa^2 \right] dA \geq 0. \quad (3.18)$$

Then, we obtain Eq. (3.13) by integrating Eq. (3.18) over y in the range $0 \leq y < \infty$. \square

Note that m_{ext} is a measure of the total rest mass of the matters and gravitational waves in the region between $y = 0$ and infinity and $\bar{\rho}_{\text{tot}}(y)$ is the surface-averaged total energy density. Since the fact that $\mathcal{R}_A \propto e^{y/2}$ in IMCF gives $2\pi \int dy \mathcal{R}_A^3 = (4\pi/3)\mathcal{R}_A^3$, the definition of Eq. (3.14) is merely natural. Note that ρ_{gw} can be interpreted as the energy density of gravitational waves¹. Since the right-hand side of Eq. (3.18) is non-negative, this inequality gives the so-called Geroch monotonicity.

For later discussions, we define the area-averaged quasilocal angular momentum.

Definition 3.4 (area-averaged quasilocal angular momentum [14]).

$$\left(8\pi \bar{J}(y) \right)^2 := \frac{A^2}{6\pi} \int_{\sigma_y} v_a v^a dA. \quad (3.19)$$

¹We can regard Eq. (3.16) as the part of energy density of gravitational waves, i.e. $8\pi\rho_{\text{gw}} = (1/2)[(\mathcal{L}_n h_{ab})^2 + (\mathcal{L}_r h_{ab})^2]$, where h_{ab} is the induced metric of σ_y .

We also define its minimum value \bar{J}_{\min} in the range $0 \leq y < \infty$,

$$\bar{J}_{\min} := \min_{\{\sigma_y\}} \bar{J}(y). \quad (3.20)$$

Using Eqs. (3.19) and (3.20), the right-hand side of Eq. (3.13) is evaluated as

$$\begin{aligned} \frac{1}{16\pi} \int_0^\infty dy \mathcal{R}_A \int_{\sigma_y} dA v^a v_a &= \frac{3}{2} \int_0^\infty dy \frac{\bar{J}^2}{\mathcal{R}_A^3} \\ &\geq \frac{3}{2} \bar{J}_{\min}^2 \int_0^\infty \frac{dy}{\mathcal{R}_A^3} = \frac{\bar{J}_{\min}^2}{\mathcal{R}_{A0}^3}, \end{aligned} \quad (3.21)$$

where we used the fact that $\mathcal{R}_A = \mathcal{R}_{A0} e^{y/2}$ holds in the IMCF. Thus, the right-hand side of Eq. (3.13) is bounded by the area-averaged quasilocal angular momentum defined by Definition 3.4.

Note that the definition of the area-averaged angular momentum (3.19) comes from the observation for spherically symmetric cases and asymptotic behavior. In this sense, the validity of the definition for general cases is far from canonical one based on conservation.

3.1.2 Some radii in axisymmetric spacetimes

At the beginning of this chapter, we mentioned that Anglada proved the refined Penrose-like inequality for the minimal surface in vacuum and axisymmetric spacetimes. In Sec. 2.4, we defined the Komar angular momentum $J(y)$ of σ_y (See Definition 2.9) and it is known that $J(y)$ is conserved with respect to y in axisymmetric vacuum cases. Following Ref. [13], for our later discussions, let us define two types of radii in axisymmetric spacetimes and then we will present some of their features.

Definition 3.5 ([14]). For axisymmetric spacelike hypersurface Σ , the radii, $\mathcal{R}_\phi(y)$ and $\mathcal{R}(y)$ are defined by

$$\frac{8\pi}{3} \mathcal{R}_\phi^4 := \int_{\sigma_y} \phi_a \phi^a dA, \quad (3.22)$$

$$\frac{1}{\mathcal{R}^2} := \frac{3}{2} \mathcal{R}_A \int_y^\infty \frac{\mathcal{R}_A}{\mathcal{R}_\phi^4} dy', \quad (3.23)$$

where ϕ^a is the axisymmetric Killing vector.

Using them, the right-hand side of Eq. (3.13) can be rewritten as

$$\frac{1}{16\pi} \int_0^\infty dy \mathcal{R}_A \int_{\sigma_y} dA v^a v_a \geq \frac{J^2}{\mathcal{R}_0^2 \mathcal{R}_{A0}}, \quad (3.24)$$

where $\mathcal{R}_0 := \mathcal{R}(0)$ and we used the following inequality obtained through the Cauchy-Schwarz inequality and the Komar angular momentum (See Definition 2.9),

$$\int_{\sigma_y} v^a v_a dA \int_{\sigma_y} \phi^a \phi_a dA \geq \left(\int_{\sigma_y} v^a \phi_a dA \right)^2 = (8\pi J)^2. \quad (3.25)$$

For spherically symmetric cases, \mathcal{R}_ϕ and \mathcal{R} coincide with the area radius \mathcal{R}_A , that is, $\mathcal{R} = \mathcal{R}_\phi = \mathcal{R}_A$. Furthermore, for a convex σ_y , we have the following feature.

Proposition 3.6 ([14]). *We assume that Σ is an axisymmetric spacelike hypersurface equipped with the inverse mean curvature flow $\{\sigma_y\}_{y \in \mathbb{R}}$. We suppose that each leaf σ_y is homeomorphic to a two-surface. For a convex σ_y , we have*

$$\frac{1}{3} \leq \frac{\mathcal{R}_A^2 \mathcal{R}^2}{\mathcal{R}_\phi^4} \leq \frac{5}{3}. \quad (3.26)$$

Proof. Following Eq. (23) in Ref. [13], in IMCF, using $A \propto e^y$, we have

$$\frac{d}{dy} \left(\frac{A^{1/2}}{\int_{\sigma_y} \phi_a \phi^a dA} \right) = -\frac{5}{2} \frac{A^{1/2}}{\int_{\sigma_y} \phi_a \phi^a dA} + \frac{2A^{1/2}}{\left(\int_{\sigma_y} \phi_a \phi^a dA \right)^2} \int_{\sigma_y} \frac{\lambda_\theta}{k} \phi_a \phi^a dA, \quad (3.27)$$

$$= -\frac{1}{2} \frac{A^{1/2}}{\int_{\sigma_y} \phi_a \phi^a dA} - \frac{2A^{1/2}}{\left(\int_{\sigma_y} \phi_a \phi^a dA \right)^2} \int_{\sigma_y} \frac{\lambda_\phi}{k} \phi_a \phi^a dA \quad (3.28)$$

where λ_ϕ is the principal curvature of σ_y in the direction of the Killing vector ϕ^a , λ_θ is the other principal curvature of σ_y , so that $k = \lambda_\theta + \lambda_\phi$, and we used the fact that $\partial_y(\phi_a \phi^a) = 2\varphi \lambda_\phi \phi_a \phi^a = 2(\lambda_\phi/k) \phi_a \phi^a$ [26].

For a convex σ_y , that is, $\lambda_\theta > 0, \lambda_\phi > 0$, Eqs. (3.27) and (3.28) lead us to

$$-\frac{5}{2} \frac{\mathcal{R}_A}{\mathcal{R}_\phi^4} \leq \frac{d}{dy} \left(\frac{\mathcal{R}_A}{\mathcal{R}_\phi^4} \right) \quad (3.29)$$

and

$$\frac{d}{dy} \left(\frac{\mathcal{R}_A}{\mathcal{R}_\phi^4} \right) \leq -\frac{1}{2} \frac{\mathcal{R}_A}{\mathcal{R}_\phi^4}, \quad (3.30)$$

respectively, and then,

$$-\frac{5}{2} \frac{\mathcal{R}_A}{\mathcal{R}_\phi^4} \leq \frac{d}{dy} \left(\frac{\mathcal{R}_A}{\mathcal{R}_\phi^4} \right) \leq -\frac{1}{2} \frac{\mathcal{R}_A}{\mathcal{R}_\phi^4}. \quad (3.31)$$

Finally, its integration over y and Eq. (3.23) in Definition 3.5 give us Eq. (3.26). \square

If the shape of σ_y is oblate or prolate, one can also show the magnitude relation between \mathcal{R}_ϕ and \mathcal{R}_A .

Proposition 3.7 ([14]). *In the same setup and under the same assumption as those in Proposition 3.6, for $\lambda_\theta \geq \lambda_\phi > 0$ (oblate case)*

$$\mathcal{R}_\phi \geq \mathcal{R}_A \quad (3.32)$$

holds, while for $0 < \lambda_\theta \leq \lambda_\phi$ (prolate case)

$$\mathcal{R}_\phi \leq \mathcal{R}_A \quad (3.33)$$

holds.

Proof. In a way similar to the derivation for Eq. (3.27), we see that

$$\frac{d}{dy} \left(\frac{A^2}{\int_{\sigma_y} \phi_a \phi^a dA} \right) = \frac{A^2}{\left(\int_{\sigma_y} \phi_a \phi^a dA \right)^2} \int_{\sigma_y} \frac{\lambda_\theta - \lambda_\phi}{k} \phi_a \phi^a dA \quad (3.34)$$

holds. For $\lambda_\theta \geq \lambda_\phi > 0$ (oblate), its integration over y gives us

$$\frac{\mathcal{R}_A}{\mathcal{R}_\phi} \leq \frac{\mathcal{R}_A}{\mathcal{R}_\phi} \Big|_{y \rightarrow \infty} = 1, \quad (3.35)$$

where we used $\mathcal{R}_A/\mathcal{R}_\phi \rightarrow 1$ at spatial infinity. On the other hand, for $0 < \lambda_\theta \leq \lambda_\phi$ (prolate), we have

$$1 \leq \frac{\mathcal{R}_A}{\mathcal{R}_\phi}. \quad (3.36)$$

□

We show the magnitude relation between the area-averaged angular momentum \bar{J} and the Komar angular momentum for vacuum and axisymmetric cases. From the definition (3.19) and the Cauchy-Schwarz inequality (3.25), it is easy to see that the relation between \bar{J} and J

$$\bar{J}^2 \geq \left(\frac{\mathcal{R}_A}{\mathcal{R}_\phi} \right)^4 J^2 \quad (3.37)$$

holds. For $0 < \lambda_\theta \leq \lambda_\phi$, together with Eq. (3.33), it tells us

$$\bar{J}^2 \geq J^2. \quad (3.38)$$

3.2 Longitudinal attractive gravity probe surface

In this section, we will present two types of AGPSs as indicators of gravity, which are generalizations of the LTS [6]. We refine the areal inequalities for these AGPSs using the inequality (3.13) obtained from the monotonicity of the Geroch mass. In Subsec. 3.2.1, we reexamine the original version of the AGPS associated with its mean curvature, as introduced in Sec. 2.6. Then, we introduce a new variant of AGPS associated with its Ricci scalar in Subsec. 3.2.2.

3.2.1 LAGPS associated with mean curvature (LAGPS-k)

In Sec. 2.6, we introduced the original AGPS (Definition 2.17) and discussed the Penrose-like inequality (Theorem 2.18). The AGPS was defined by comparing the derivative of the mean curvature k along the longitudinal direction and k^2 in order to characterize the strength of gravity. Then, we name it the longitudinal attractive gravity probe surface associated with mean curvature (LAGPS-k), to differentiate it from the three additional types of AGPS that will be presented in subsequent sections. For the sake of completeness, we will reiterate the definition of LAGPS-k here.

Definition 3.8 (longitudinal attractive gravity probe surface associated with mean curvature [8, 14, 15]). In the same setup as those in Subsec. 2.5.2, a longitudinal attractive gravity probe surface associated with mean curvature (LAGPS-k) is defined by a compact two-surface satisfying $k > 0$ and

$${}^{(3)}\mathcal{L}_r k \geq \alpha k^2, \quad (3.39)$$

where α is a constant greater than $-1/2$.

For the LAGPS-k, Lemma 3.3 gives us the following theorem.

Theorem 3.9 ([14, 15]). *We assume that spacetime M satisfies the Einstein equation (2.2) and Σ is an asymptotically flat spacelike maximal hypersurface equipped with the inverse mean curvature flow $\{\sigma_y\}_{y \in \mathbb{R}}$ where σ_0 is an LAGPS- k . We suppose that each leaf σ_y is homeomorphic to a two-surface. If $\rho := T_{ab}n^a n^b \geq 0$ holds where n^a is the future-directed unit normal vector to Σ , the following inequality for the LAGPS- k σ_0 holds*

$$\begin{aligned} m_{\text{ADM}} - \left(m_{\text{ext}} + \frac{3}{3+4\alpha} m_{\text{int}} \right) &\geq \frac{1+2\alpha}{3+4\alpha} \mathcal{R}_{A0} + \frac{1}{\mathcal{R}_{A0}^3} \left(\bar{J}_{\text{min}}^2 + \frac{3}{3+4\alpha} \bar{J}_0^2 \right) \\ &\geq \frac{1+2\alpha}{3+4\alpha} \mathcal{R}_{A0} + 2 \frac{3+2\alpha}{3+4\alpha} \frac{\bar{J}_{\text{min}}^2}{\mathcal{R}_{A0}^3}, \end{aligned} \quad (3.40)$$

where $\mathcal{R}_{A0} = \sqrt{A_0/4\pi}$ with the area of σ_0 , A_0 and

$$m_{\text{int}} := \frac{4\pi}{3} \mathcal{R}_{A0}^3 \bar{\rho}_{\text{tot}}(0). \quad (3.41)$$

Proof. On the maximal slice Σ , the surface integral of Eq. (3.3) over the LAGPS- k σ_0 with the condition of Eq. (3.39) in the definition of the LAGPS- k implies

$$\left(1 + \frac{4}{3}\alpha \right) \int_{\sigma_0} dA k^2 \leq \frac{16\pi}{3} - \frac{2}{3} \int_{\sigma_0} dA (16\pi \rho_{\text{tot}} + 2v_a v^a). \quad (3.42)$$

Using \bar{J} defined by Eq. (3.19), we write Eq. (3.42) as

$$\left(1 + \frac{4}{3}\alpha \right) \int_{\sigma_0} dA k^2 \leq \frac{16\pi}{3} - \frac{32\pi}{3} A_0 \bar{\rho}_{\text{tot}0} - 32\pi \frac{\bar{J}_0^2}{\mathcal{R}_{A0}^4}. \quad (3.43)$$

For the last term in the right-hand side of Eq. (3.13), we use the fact that Eq. (3.21) holds. Then, with simple manipulation, we can see that Eqs. (3.13) and (3.43) imply Eq. (3.40). \square

Note that m_{int} defined by Eq. (3.41) may be regarded as a mass in the region surrounded by σ_0 .

We mentioned that LAGPS- k is the extension from the LTS, and characterize the strength of gravity by setting the parameter α . For an LTS ($\alpha = 0$), Eq. (3.40) becomes

$$m_{\text{ADM}} - (m_{\text{ext}} + m_{\text{int}}) \geq \frac{\mathcal{R}_{A0}}{3} + \frac{\bar{J}_0^2 + \bar{J}_{\text{min}}^2}{\mathcal{R}_{A0}^3} \geq \frac{\mathcal{R}_{A0}}{3} + 2 \frac{\bar{J}_{\text{min}}^2}{\mathcal{R}_{A0}^3}. \quad (3.44)$$

This includes the inequality (2.68), $m_{\text{ADM}} \geq \mathcal{R}_{A0}/3$ obtained in Ref. [6]. For a $k = 0$ surface ($\alpha \rightarrow \infty$), Eq. (3.40) becomes

$$m_{\text{ADM}} - m_{\text{ext}} \geq \frac{\mathcal{R}_{A0}}{2} + \frac{\bar{J}_{\text{min}}^2}{\mathcal{R}_{A0}^3}. \quad (3.45)$$

From this, one can obtain the Penrose inequality, $m_{\text{ADM}} \geq \mathcal{R}_{A0}/2$, shown in Ref. [10] (See also Refs. [11, 12]). By taking the square of Eq. (3.45),

$$(m_{\text{ADM}} - m_{\text{ext}})^2 \geq \left(\frac{\mathcal{R}_{A0}}{2} \right)^2 + \frac{\bar{J}_{\text{min}}^2}{\mathcal{R}_{A0}^2} + \left(\frac{\bar{J}_{\text{min}}^2}{\mathcal{R}_{A0}^3} \right)^2 \geq \left(\frac{\mathcal{R}_{A0}}{2} \right)^2 + \frac{\bar{J}_{\text{min}}^2}{\mathcal{R}_{A0}^2}. \quad (3.46)$$

Since we can see that the equality of Eq. (3.46) is exactly same with Eq. (2.53):

$$m^2 = \left(\frac{\mathcal{R}}{2} \right)^2 + \frac{J^2}{\mathcal{R}^2} = \frac{A}{16\pi} + 4\pi \frac{J^2}{A},$$

Eq. (3.46) gives us the refined Penrose inequality (1.2) taking account of the angular momentum.

The arithmetic-geometric mean of the right-hand side of Eq. (3.40) gives us a corollary.

Corollary 3.10 ([14]). *In the same setup and under the same assumption as those in Theorem 3.9,*

$$\Delta m_{\text{ADM}} \geq 2C_\alpha \frac{\bar{J}_{\text{min}}}{\mathcal{R}_{A0}} \quad (3.47)$$

holds for LAGPS- k , where

$$\Delta m_{\text{ADM}} := m_{\text{ADM}} - \left(m_{\text{ext}} + \frac{3}{3+4\alpha} m_{\text{int}} \right) \quad (3.48)$$

and

$$C_\alpha := \sqrt{\frac{2(1+2\alpha)(3+2\alpha)}{(3+4\alpha)^2}}. \quad (3.49)$$

This corollary gives the lower bound for \mathcal{R}_{A0} as

$$\mathcal{R}_{A0} \geq 2C_\alpha \frac{\bar{J}_{\text{min}}}{\Delta m_{\text{ADM}}}. \quad (3.50)$$

It is interesting to compare it to the universal inequality $\mathcal{R} \gtrsim J^{1/2}$ for an axisymmetric rotating body shown by Dain [27] (See also Refs. [28, 29]). The ratio ϵ_α of the lower bound for \mathcal{R}_{A0} to Dain's one is

$$\epsilon_\alpha \sim \frac{J/m}{J^{1/2}} \sim a^{1/2}, \quad (3.51)$$

where $a := J/m^2$ is the Kerr parameter. For astrophysical objects except for compact objects, a is much larger than unity. Therefore, our inequality is relatively strong for such cases.

In the limit of $\alpha = -1/2$, $C_{-1/2}$ vanishes and thus the inequality (3.50) does not give any constraint. Going back to the original inequality (3.40), however, we can give another lower bound on \mathcal{R}_{A0} . Since the first term in the right-hand side of the inequality (3.40) is non-negative for $\alpha \geq -1/2$, we have a weaker inequality,

$$m_{\text{ADM}} - \left(m_{\text{ext}} + \frac{3}{3+4\alpha} m_{\text{int}} \right) \geq 2 \frac{3+2\alpha}{3+4\alpha} \frac{\bar{J}_{\text{min}}^2}{\mathcal{R}_{A0}^3}. \quad (3.52)$$

Due to the fact that $m_{\text{ext}} \geq 0$, $m_{\text{int}} \geq 0$, we have

$$m_{\text{ADM}} \geq 2 \frac{3+2\alpha}{3+4\alpha} \frac{\bar{J}_{\text{min}}^2}{\mathcal{R}_{A0}^3}. \quad (3.53)$$

This is rearranged to

$$\mathcal{R}_{A0} \geq \left(2 \frac{3+2\alpha}{3+4\alpha} \frac{\bar{J}_{\text{min}}^2}{m_{\text{ADM}}} \right)^{1/3}. \quad (3.54)$$

Contrasted to Eq. (3.50), this inequality gives a meaningful condition for $\alpha = -1/2$. We could have the lower bound of Eq. (3.54) for the areal radius of LAGPS- k with $\alpha = -1/2$ and $\epsilon_{-1/2} \sim (J^{2/3}/m^{1/3})/J^{1/2} \sim a^{1/6}$.

For vacuum and axisymmetric spacetimes, we rewrote the right-hand side of the key formula (3.13) using Eq. (3.24), which is bounded by using the Komar angular momentum. Thus, for the LAGPS- k , one has the following theorem.

Theorem 3.11 ([14, 15]). *Let M be a vacuum and axisymmetric spacetime satisfying the Einstein equation (2.2), and Σ be an asymptotically flat axisymmetric spacelike maximal hypersurface equipped with the inverse mean curvature flow $\{\sigma_y\}_{y \in \mathbb{R}}$ where σ_0 is an LAGPS- k .*

We suppose that each leaf σ_y is homeomorphic to a two-surface. Then, we have an inequality for the LAGPS- k σ_0 ,

$$m_{\text{ADM}} - \left(m_{\text{gw}}^{(\text{ext})} + \frac{3}{3+4\alpha} m_{\text{gw}}^{(\text{int})} \right) \geq \frac{1+2\alpha}{3+4\alpha} \mathcal{R}_{A0} + \frac{1+\chi_\alpha}{\mathcal{R}_0^2 \mathcal{R}_{A0}} J^2, \quad (3.55)$$

where

$$\chi_\alpha := \frac{3}{3+4\alpha} \frac{\mathcal{R}_0^2 \mathcal{R}_{A0}^2}{\mathcal{R}_{\phi_0}^4}, \quad (3.56)$$

$$m_{\text{gw}}^{(\text{ext})} := 2\pi \int_0^\infty dy \mathcal{R}_A^3 \bar{\rho}_{\text{gw}}, \quad (3.57)$$

$$m_{\text{gw}}^{(\text{int})} := \frac{4\pi}{3} \mathcal{R}_{A0}^3 \bar{\rho}_{\text{gw}}(0) \quad (3.58)$$

and

$$\bar{\rho}_{\text{gw}}(y) := \frac{1}{A} \int_{\sigma_y} dA \rho_{\text{gw}}. \quad (3.59)$$

Since Eq. (3.26) holds for a convex σ_y in the IMCF, χ_α is bounded as

$$\frac{1}{3+4\alpha} \leq \chi_\alpha \leq \frac{5}{3+4\alpha}. \quad (3.60)$$

Note that Eqs. (3.40) and (3.55) hold even for $-1/2 > \alpha > -3/4$. However, bearing the bound for the area in mind, we have imposed $\alpha > -1/2$ in Definition 3.8.

For an LTS ($\alpha = 0$), Eq. (3.55) becomes

$$m_{\text{ADM}} - (m_{\text{gw}}^{(\text{ext})} + m_{\text{gw}}^{(\text{int})}) \geq \frac{\mathcal{R}_{A0}}{3} + (1+\chi_0) \frac{J^2}{\mathcal{R}_0^2 \mathcal{R}_{A0}}. \quad (3.61)$$

For a surface which has the zero mean curvature ($\alpha \rightarrow \infty$), we recover Anglada's result (Theorem 2.10)

$$m_{\text{ADM}} - m_{\text{gw}}^{(\text{ext})} \geq \frac{\mathcal{R}_{A0}}{2} + \frac{J^2}{\mathcal{R}_0^2 \mathcal{R}_{A0}}. \quad (3.62)$$

Applying the arithmetic-geometric mean for Eq. (3.55), we also have a similar result to Corollary 3.10.

Corollary 3.12 ([14, 15]). *In the same setup and assumption as Theorem 3.11,*

$$m_{\text{ADM}} - \left(m_{\text{gw}}^{(\text{ext})} + \frac{3}{3+4\alpha} m_{\text{gw}}^{(\text{int})} \right) \geq 2F_\alpha \frac{|J|}{\mathcal{R}_0} \quad (3.63)$$

holds for an LAGPS- k , where

$$F_\alpha := \sqrt{\frac{(1+\chi_\alpha)(1+2\alpha)}{3+4\alpha}}. \quad (3.64)$$

Note that F_α depends on radii (See the definition of χ_α , Eq. (3.56)). For convex σ_y , however, Eq. (3.60) for χ_α gives a lower bound of F_α as $F_\alpha \geq 2\sqrt{(1+\alpha)(1+2\alpha)/(3+4\alpha)^2} =: F_{\text{min}}$. Since F_{min} is independent of radii, Eq. (3.63) gives a lower bound for \mathcal{R}_0 of AGPS,

$$\mathcal{R}_0 \geq 2F_{\text{min}} \frac{|J|}{m_{\text{ADM}}}. \quad (3.65)$$

In the limit of $\alpha = -1/2$, one can have a similar lower bound for a combination of radii, but its form is not simple. Since the argument based on the order of magnitude is the same with that in the previous section, here we do not show the derivation again.

We also point out that, applying the arithmetic-geometric mean after taking the square for the inequality of Eq. (3.55), we have

$$\begin{aligned}
m_{\text{ADM}}^2 &\geq \left(\frac{1+2\alpha}{3+4\alpha} \mathcal{R}_{A0} \right)^2 + 2(1+\chi_\alpha) \frac{1+2\alpha}{3+4\alpha} \frac{J^2}{\mathcal{R}_0^2} + \left(\frac{1+\chi_\alpha}{\mathcal{R}_0^2 \mathcal{R}_{A0}} J^2 \right)^2 \\
&\geq \left(\frac{1+2\alpha}{3+4\alpha} \mathcal{R}_{A0} \right)^2 + 2(1+\chi_\alpha) \frac{1+2\alpha}{3+4\alpha} \frac{J^2}{\mathcal{R}_0^2} \\
&\geq \eta_\alpha \frac{\mathcal{R}_{A0}}{\mathcal{R}_0} |J|,
\end{aligned} \tag{3.66}$$

where

$$\eta_\alpha := \left[\frac{2(1+2\alpha)}{3+4\alpha} \right]^{3/2} (1+\chi_\alpha)^{1/2}. \tag{3.67}$$

For the prolate LAGPS-k, we can show

$$\begin{aligned}
\left(\frac{\mathcal{R}_{A0}}{\mathcal{R}_0} \right)^2 &= \frac{3}{2} \mathcal{R}_{A0}^3 \int_0^\infty \frac{\mathcal{R}_A^4}{\mathcal{R}_\phi^4} \frac{1}{\mathcal{R}_A^3} dy \\
&\geq \frac{3}{2} \mathcal{R}_{A0}^3 \int_0^\infty \frac{1}{\mathcal{R}_A^3} dy \\
&= 1,
\end{aligned} \tag{3.68}$$

where we used Proposition 3.7 that $\mathcal{R}_A/\mathcal{R}_\phi \geq 1$ holds for the prolate LAGPS-k in the second line and $\mathcal{R}_A = \mathcal{R}_{A0} e^{y/2}$ in the third line. Then, Eq. (3.66) gives us

$$m_{\text{ADM}} \geq \eta_\alpha^{1/2} |J|^{1/2}. \tag{3.69}$$

For the limit $\alpha \rightarrow \infty$ where the LAGPS-k approaches the $k = 0$ surface, this inequality reduces to $m_{\text{ADM}} \geq |J|^{1/2}$. This inequality has been shown in a different way by the authors of Refs. [30, 31] for spacetimes close to the extreme Kerr solution.

3.2.2 LAGPS associated with Ricci scalar (LAGPS-r)

Here, we present the variant from the original version of the AGPS. Let us reconsider Eq. (2.67) for the radial derivative of the mean curvature in the Schwarzschild case. Then, we realize that one can relate the factor $2/r^2$ in the right-hand side to the two-dimensional Ricci scalar ${}^{(2)}R$. Thus, one can also define an attractive gravity probe surface associated with Ricci scalar ${}^{(2)}R$ as follows.

Definition 3.13 (longitudinal attractive gravity probe surface associated with Ricci scalar [15]). In the same setup as those in Subsec. 2.5.2, a longitudinal attractive gravity probe surface associated with Ricci scalar ${}^{(2)}R$ (LAGPS-r) is defined by a compact two-surface satisfying $k > 0$ and

$${}^{(3)}\mathcal{L}_r k \geq -{}^{(2)}R(1 - \gamma_L), \tag{3.70}$$

where γ_L is a constant.

For the Schwarzschild spacetime, the condition of Eq. (3.70) gives us

$$r \leq 3m/\gamma_L \quad (3.71)$$

for $m > 0$ and $\gamma_L > 0$. Therefore, for $\gamma_L \rightarrow +0$, the radius r of the surface can be arbitrarily large, while for $\gamma_L = 1$, the radius must be equal to or smaller than that of the photon sphere. Note that the LAGPS-r with $\gamma_L = 3/2$ corresponds to the horizon in the Schwarzschild case.

For the LAGPS-r, we have the following theorem.

Theorem 3.14 ([15]). *We assume that spacetime M satisfies the Einstein equation (2.2) and Σ is an asymptotically flat spacelike maximal hypersurface equipped with the inverse mean curvature flow $\{\sigma_y\}_{y \in \mathbb{R}}$ where σ_0 is an LAGPS-r. We suppose that each leaf σ_y is homeomorphic to a two-surface. If $\rho := T_{ab}n^a n^b \geq 0$ holds where n^a is the future-directed unit normal vector to Σ , the following inequality for the LAGPS-r σ_0 holds*

$$\begin{aligned} m_{\text{ADM}} - (m_{\text{int}} + m_{\text{ext}}) &\geq \frac{\gamma_L}{3} \mathcal{R}_{A0} + \frac{\bar{J}_0^2 + \bar{J}_{\text{min}}^2}{\mathcal{R}_{A0}^3} \\ &\geq \frac{\gamma_L}{3} \mathcal{R}_{A0} + 2 \frac{\bar{J}_{\text{min}}^2}{\mathcal{R}_{A0}^3}. \end{aligned} \quad (3.72)$$

Proof. One can show that the Willmore function, $\int_{\sigma_0} k^2 dA$, on the LAGPS-r σ_0 is bounded from above. From the surface integral of Eq. (3.3) over the LAGPS-r σ_0 and the condition of Eq. (3.70), we have

$$\begin{aligned} \int_{\sigma_0} \left[\left(-\gamma_L + \frac{3}{2} \right) {}^{(2)}R - G_{ab}n^a n^b + \kappa K_{(r)} \right. \\ \left. + \frac{1}{2} \left(\frac{1}{2} \kappa^2 - \tilde{\kappa}_{ab} \tilde{\kappa}^{ab} - \frac{3}{2} k^2 - \tilde{k}_{ab} \tilde{k}^{ab} \right) - v_a v^a - \varphi^{-2} (\mathcal{D}\varphi)^2 \right] dA \geq 0. \end{aligned} \quad (3.73)$$

From the assumptions that the Einstein equation $G_{ab} = 8\pi T_{ab}$ to hold for the spacetime M , σ_0 to be topologically sphere $\sigma_0 \approx S^2$, k to be non-negative $k \geq 0$, and Σ to be maximally sliced, i.e. $K = \kappa + K_{(r)} = 0$, Eq. (3.73) implies

$$\int_{\sigma_0} k^2 dA \leq \frac{16\pi}{3} (3 - 2\gamma_L) - \frac{2}{3} \int_{\sigma_0} \left(16\pi \rho_{\text{tot}} + 2v_a v^a + \frac{3}{2} \kappa^2 + 2\varphi^{-2} (\mathcal{D}\varphi)^2 \right) dA \quad (3.74)$$

$$\leq \frac{16\pi}{3} (3 - 2\gamma_L) - \frac{2}{3} \int_{\sigma_0} (16\pi \rho_{\text{tot}} + 2v_a v^a) dA, \quad (3.75)$$

where we used the Gauss-Bonnet theorem. Then, Eqs. (3.13), (3.21) and (3.75) give us Eq. (3.72). \square

Note that assuming the non-negativity of the energy density of matters, $\rho \geq 0$, when $\gamma_L = 3/2$, the inequality (3.74) tells us

$$k = \rho_{\text{tot}} = v_a = \kappa = \mathcal{D}_a \varphi = 0 \quad (3.76)$$

on σ_0 . Thus, we have a relatively strong consequence that σ_0 is totally geodesic in Σ since $k = 0$ and $\tilde{k}_{ab} = 0$ from $\rho_{\text{tot}} = \rho_{\text{gw}} = 0$, where ρ_{gw} is defined by Eq. (3.16).

For vacuum and axisymmetric spacetimes, Lemma 3.3 gives us the following theorem.

Theorem 3.15 ([15]). *Let M be a vacuum and axisymmetric spacetime satisfying the Einstein equation (2.2), and Σ be an asymptotically flat axisymmetric spacelike maximal hypersurface equipped with the inverse mean curvature flow $\{\sigma_y\}_{y \in \mathbb{R}}$ where σ_0 is an LAGPS-r. We suppose that each leaf σ_y is homeomorphic to a two-surface. Then, we have an inequality for the LAGPS-r σ_0 ,*

$$m_{\text{ADM}} - (m_{\text{gw}}^{(\text{int})} + m_{\text{gw}}^{(\text{ext})}) \geq \frac{\gamma_L}{3} \mathcal{R}_{A0} + \frac{1 + \chi_0}{\mathcal{R}_0^2 \mathcal{R}_{A0}} J^2, \quad (3.77)$$

where χ_0 is defined by²

$$\chi_0 := \frac{\mathcal{R}_0^2 \mathcal{R}_{A0}^2}{\mathcal{R}_{\phi 0}^4}. \quad (3.78)$$

Note that the arithmetic-geometric mean of the right-hand sides of Eqs. (3.72) and (3.77) gives us similar results to Corollaries 3.10 and 3.12. Since the argument based on the order of magnitude is the same with that in the previous subsection, here we do not show the derivation again.

For the LAGPS-r, note that one cannot discuss with the $k = 0$ surfaces. Here, we focus on the case of a $k = 0$ surface in vacuum and axisymmetric spacetimes. For an LAGPS-k with $\alpha \rightarrow \infty$ that correspond to the $k = 0$ surface, and we have Eq. (3.62):

$$m_{\text{ADM}} - m_{\text{gw}}^{(\text{ext})} \geq \frac{\mathcal{R}_{A0}}{2} + \frac{J^2}{\mathcal{R}_0^2 \mathcal{R}_{A0}}$$

from Eq. (3.55). On the other hand, for an LAGPS-r, setting $\gamma_L = 3/2$ which corresponds to the $k = 0$ surface in the case of the Schwarzschild spacetime, we have

$$m_{\text{ADM}} - m_{\text{gw}}^{(\text{ext})} \geq \frac{\mathcal{R}_{A0}}{2}, \quad (3.79)$$

where we used the fact that the angular momentum and ρ_{gw} vanishes on the LAGPS-r when $\gamma_L = 3/2$ due to the discussion around Eq. (3.76). Thus, we cannot refine the inequalities by including the contribution from the angular momentum. Therefore, the LAGPS-r does not characterize the $k = 0$ surface in a direct way.

3.3 Transverse attractive gravity probe surface

As a generalization of the photon sphere, the photon surface was introduced based on the null geodesics [5]. However, it is turned out that a geometrical constraint is required for the existence of the photon surface. Then, the DTTS has been proposed to describe wider class of spacetimes having strong gravity regions [7]. This section aims to discuss the generalizations of the DTTS to characterize weak gravity region too as the TAGPS-k/TAGPS-r. which serve to characterize the strength of gravity using an intensity parameter. Mirroring the approach of the previous section, we introduce two types of generalizations associated with the mean curvature and Ricci scalar and refine the Penrose-like inequalities for those surfaces.

3.3.1 TAGPS associated with mean curvature (TAGPS-k)

We first examine the second condition of the DTTS definition (Eq. (2.62))

$$\max(\bar{K}_{ab} k^a k^b) = 0,$$

²This is equal to the $\alpha = 0$ case of χ_α (See Eq. (3.56)).

where \bar{K}_{ab} is the extrinsic curvature of S , and k^a is an arbitrary null tangent vector to S . Eq. (2.62) characterizes the behavior of null geodesics emitting from σ_0 . In this subsection, we propose a modification to the second condition of Eq. (2.62) to characterize weak gravity region as well as strong gravity one. This leads to the introduction of a new surface. We refer to this surface as the transverse attractive gravity probe surface associated with mean curvature (TAGPS-k).

Before introducing the TGAPS-k, for later discussion, we point out that the left-hand side of Eq. (2.62) satisfies the following inequality.

Proposition 3.16 ([15]). *In the same setup as those in Subsec. 2.5.2, let \bar{K}_{ab} be the extrinsic curvature of S with respect to the spacelike normal vector r^a and k be the mean curvature of σ_0 , then*

$$\max(\bar{K}_{ab}k^ak^b) \geq \bar{K}_{(n)} + \frac{1}{2}k, \quad (3.80)$$

where k^a is an arbitrary null tangent vector to S and $\bar{K}_{(n)} := \bar{K}_{ab}n^an^b$.

Proof. In general, with a timelike unit vector n^a orthogonal to σ_0 and a spacelike unit vector s^a tangent to σ_0 , the null tangent vector to S can be given by $k^a = n^a + s^a$, and hence, the left-hand side of Eq. (2.62) is evaluated as

$$\begin{aligned} \max(\bar{K}_{ab}k^ak^b) &= \max(\bar{K}_{(n)} + k_{ab}s^as^b - 2s^av_a) \\ &= \bar{K}_{(n)} + \frac{1}{2}k + \max(\tilde{k}_{ab}s^as^b - 2s^av_a) \\ &\geq \bar{K}_{(n)} + \frac{1}{2}k + \max(\tilde{k}_{ab}s^as^b). \end{aligned} \quad (3.81)$$

Here, n^a is fixed and one takes the maximum among various s^a in the S^1 direction in the second and the third lines. In deriving the third line, we used the fact that for $\pm s^a$ which give $\max(\tilde{k}_{ab}s^as^b)$, one of $\max[\tilde{k}_{ab}s^as^b - 2(\pm s^a)v_a]$ must be equal to or greater than $\max(\tilde{k}_{ab}s^as^b)$. Since k_{ab} is symmetric tensor, there is the orthogonal basis $\{e_1, e_2\}$ such that $k_{ab} = k_1(e_1)_a(e_1)_b + k_2(e_2)_a(e_2)_b$. Then,

$$\tilde{k}_{ab}s^as^b = (k_1 - k_2)\frac{\cos(2\theta)}{2}, \quad (3.82)$$

where s^a is parametrized as $s^a = \cos\theta(e_1)^a + \sin\theta(e_2)^a$. Thus, we find

$$\max(\tilde{k}_{ab}s^as^b) = \frac{\max(k_1, k_2) - \min(k_1, k_2)}{2} \geq 0, \quad (3.83)$$

and hence, we obtain Eq. (3.80). \square

As a trial for the extension of the DTTS to include an intensity parameter for gravity, instead of the condition of Eq. (2.62), we may impose

$$\max(\bar{K}_{ab}k^ak^b) \leq -\beta k \quad (3.84)$$

and β is a constant larger than $-1/2$. Using Eq. (3.80) seen in Proposition 3.16, Eq. (3.84) leads to

$$\bar{K}_{(n)} \leq -\frac{2\beta + 1}{2}k. \quad (3.85)$$

For the Schwarzschild spacetime, Eq. (3.85) gives us

$$r \leq \frac{3 + 4\beta}{1 + 2\beta}m. \quad (3.86)$$

It is easy to see that the coefficient of the right-hand side is monotonically decreasing function of β . The right-hand side becomes $2m$ for the limit of $\beta \rightarrow \infty$ and $3m$ for the $\beta = 0$ case. Since we can regard β in Eq. (3.84) as an intensity parameter for gravity, we will adopt the condition of Eq. (3.84) instead of Eq. (2.62) for the TAGPS-k. Note that the null tangent k^a must be normalized as the above argument for the Schwarzschild spacetime.

Definition 3.17 (transverse attractive gravity probe surface associated with mean curvature [15]). In the same setup as those in Subsec. 2.5.2, a TAGPS-k σ_0 is defined by a compact two-surface satisfying the three conditions:

$$\kappa = 0, \quad (3.87)$$

$$\max(\bar{K}_{ab}k^ak^b) \leq -\beta k, \quad (3.88)$$

$${}^{(3)}\bar{\mathcal{L}}_n\kappa \leq 0, \quad (3.89)$$

where β is a constant greater than $-1/2$, k^a is an arbitrary null tangent vector to S such that $p_{ab}k^b = n_a$ holds, and the lapse function N is taken to be constant on σ_0 .

For the TAGPS-k, Lemma 3.3 gives us the following theorem.

Theorem 3.18 ([15]). *We assume that M satisfies the Einstein equation (2.2) and Σ is an asymptotically flat spacelike maximal hypersurface equipped with the inverse mean curvature flow $\{\sigma_y\}_{y \in \mathbb{R}}$ where σ_0 is an TAGPS-k with $k \geq 0$. We suppose that each leaf σ_y is homeomorphic to a two-surface. If $\rho := T_{ab}n^an^b \geq 0$ holds where n^a is the future-directed unit normal vector to Σ , the following inequality for the TAGPS-k σ_0 holds*

$$\begin{aligned} m_{\text{ADM}} + \frac{3}{3+4\beta} p_r^{(\text{int})} - m_{\text{ext}} &\geq \frac{1+2\beta}{3+4\beta} \mathcal{R}_{A0} + \frac{1}{\mathcal{R}_{A0}^3} \left(\frac{3}{3+4\beta} \bar{J}_0^2 + \bar{J}_{\min}^2 \right) \\ &\geq \frac{1+2\beta}{3+4\beta} \mathcal{R}_{A0} + 2 \frac{3+2\beta}{3+4\beta} \frac{\bar{J}_{\min}^2}{\mathcal{R}_{A0}^3}, \end{aligned} \quad (3.90)$$

where

$$p_r^{(\text{int})} := \frac{4\pi}{3} \mathcal{R}_{A0}^3 \bar{P}_{r0}^{(\text{tot})}. \quad (3.91)$$

And $\bar{P}_{r0}^{(\text{tot})}$ is the surface-averaged one for the total radial pressure $P_r^{(\text{tot})} = P_r + P_r^{(\text{gw})}$,

$$\bar{P}_{r0}^{(\text{tot})} = \frac{1}{A_0} \int_{\sigma_0} P_r^{(\text{tot})} dA, \quad (3.92)$$

where $P_r := T_{ab}r^ar^b$ and

$$8\pi P_r^{(\text{gw})} = \frac{1}{2} (\tilde{k}_{ab}\tilde{k}^{ab} + \tilde{\kappa}_{ab}\tilde{\kappa}^{ab}) = 8\pi\rho_{\text{gw}}. \quad (3.93)$$

Proof. Considering the surface integral of Eq. (3.8) over σ_0 and then, using the inequality of Eq. (3.85), which originates from the condition of Eq. (3.88), we have

$$\int_{\sigma_0} \left[-\frac{1}{2} {}^{(2)}R - G_{ab}r^ar^b + \left(\beta + \frac{3}{4} \right) k^2 - \frac{1}{2} (\tilde{k}_{ab}\tilde{k}^{ab} + \tilde{\kappa}_{ab}\tilde{\kappa}^{ab}) + v_a v^a \right] dA \leq 0, \quad (3.94)$$

where we used the fact that the time lapse function N is constant³ on σ_0 and k is non-negative on σ_0 so that

$$\int_{\sigma_0} k \bar{K}_{(n)} dA \leq -\frac{2\beta+1}{2} \int_{\sigma_0} k^2 dA. \quad (3.96)$$

Note that on σ_0 , κ_{ab} is a traceless quantity because of the condition of Eq. (3.87), i.e., $\kappa_{ab} = \tilde{\kappa}_{ab}$. From the assumption that Einstein equation $G_{ab} = 8\pi T_{ab}$ to hold for the spacetime (M, g_{ab}) and σ_0 to be topologically sphere $\sigma_0 \approx S^2$, Eq. (3.94) implies

$$\left(1 + \frac{4}{3}\beta\right) \int_{\sigma_0} k^2 dA \leq \frac{16\pi}{3} + \frac{2}{3} \int_{\sigma_0} (16\pi P_r^{(\text{tot})} - 2v_a v^a) dA. \quad (3.97)$$

Then, Lemma 3.3, with Eqs. (3.21) and (3.97), gives us Eq. (3.90). \square

Note that in the limit of $\beta \rightarrow \infty$, we can see that $k = 0$ holds on σ_0 . This consequence is directly expected from Eq. (3.88).

In vacuum and axisymmetric cases, we obtain the following areal inequality for the TAGPS-k.

Theorem 3.19 ([15]). *Let M be a vacuum and axisymmetric spacetime satisfying the Einstein equation (2.2), and Σ be an asymptotically flat axisymmetric spacelike maximal hypersurface equipped with the inverse mean curvature flow $\{\sigma_y\}_{y \in \mathbb{R}}$ where σ_0 is an TAGPS-k with $k \geq 0$. We suppose that each leaf σ_y is homeomorphic to a two-surface. Then, we have an inequality for the TAGPS-k σ_0 ,*

$$m_{\text{ADM}} + \frac{3}{3+4\beta} p_{\text{gw}}^{(\text{int})} - m_{\text{gw}}^{(\text{ext})} \geq \frac{1+2\beta}{3+4\beta} \mathcal{R}_{A0} + \frac{1+\chi_\beta}{\mathcal{R}_0^2 \mathcal{R}_{A0}} J^2, \quad (3.98)$$

where

$$\chi_\beta := \frac{3}{3+4\beta} \frac{\mathcal{R}_0^2 \mathcal{R}_{A0}^2}{\mathcal{R}_{\phi_0}^4} \quad (3.99)$$

and

$$p_{\text{gw}}^{(\text{int})} := \frac{4\pi}{3} \mathcal{R}_{A0}^3 \bar{P}_{r0}^{(\text{gw})}. \quad (3.100)$$

Since χ_β has the same expression as χ_α introduced in Eq. (3.55), the same constraint as Eq. (3.60) holds but α is replaced by β . Again, the arithmetic-geometric mean of the right-hand sides of Eqs. (3.90) and (3.98) gives us the results similar to Corollaries 3.10 and 3.12.

3.3.2 TAGPS associated with Ricci scalar (TAGPS-r)

In this subsection, we give another extension of the DTTS to characterize the weak gravity too. In contrast to the TAGPS-k, we keep the two conditions (2.61) and (2.62) in Definition 2.13

$$\begin{aligned} \kappa &= 0, \\ \max(\bar{K}_{ab} k^a k^b) &= 0, \end{aligned}$$

³Inequality (3.94) is achieved even if N is not constant, because the contribution involving N is positive,

$$\int_{\sigma_0} N^{-1} \mathcal{D}^2 N dA = \int_{\sigma_0} (N^{-1} \mathcal{D}N)^2 dA \geq 0. \quad (3.95)$$

Therefore, Theorems 3.18 and 3.19 hold even for non-constant N .

and consider the modification to the third condition (2.63)

$${}^{(3)}\bar{\mathfrak{L}}_n\kappa \leq 0.$$

For this purpose, we first examine a photon surface S of the Schwarzschild spacetime that consists of a collection of worldlines of transversely emitted photons from an $r = \text{constant}$ sphere in a $t = \text{constant}$ hypersurface, where the conditions of Eqs. (2.61) and (2.62) are satisfied. The Lie derivative of κ with respect to n^a is

$${}^{(3)}\bar{\mathfrak{L}}_n\kappa = \frac{2}{r^2} \left(1 - \frac{3m}{r} \right). \quad (3.101)$$

Therefore, the condition of Eq. (2.63) implies $r \leq 3m$. The equality of Eq. (2.63) states $r = 3m$, which is exactly the same as the location of the photon sphere of the Schwarzschild spacetime.

As a trial of extension of the DTTS to include an intensity parameter for gravity strength, instead of the condition of Eq. (2.63), we impose

$${}^{(3)}\bar{\mathfrak{L}}_n\kappa \leq {}^{(2)}R(1 - \gamma_T), \quad (3.102)$$

where γ_T is a constant. For the Schwarzschild spacetime, this condition is reduced to

$$r \leq \frac{3m}{\gamma_T}. \quad (3.103)$$

Therefore, in the limit $\gamma_T \rightarrow +0$, r can be arbitrarily large, and $r \leq 3m$ for the $\gamma_T = 1$ case, and $r \leq 2m$ for the $\gamma_T = 3/2$ case. The parameter γ_T in Eq. (3.102) is regarded as the intensity parameter for gravity. For this reason, we will adopt the condition of Eq. (3.102) instead of Eq. (2.63) for the new definition of the TAGPS, which we call the transverse AGPS associated with Ricci scalar (TAGPS-r).

Definition 3.20 (transverse attractive gravity probe surface associated with Ricci scalar [15]). In the same setup as those in Subsec. 2.5.2, a TAGPS-r σ_0 is defined by a compact two-surface satisfying the three conditions:

$$\kappa = 0, \quad (3.104)$$

$$\max(\bar{K}_{ab}k^ak^b) = 0, \quad (3.105)$$

$${}^{(3)}\bar{\mathfrak{L}}_n\kappa \leq {}^{(2)}R(1 - \gamma_T), \quad (3.106)$$

where γ_T is a constant. k^a is an arbitrary null tangent vector to S such that $p_{ab}k^b = n_a$ holds, and the lapse function N is taken to be constant on σ_0 .

Here, several remarks are added. In the above definition, the quantity k (the trace of the extrinsic curvature of σ_0 in the spacelike hypersurface Σ) is not used. In this sense, the concept of the TAGPS-r is free from the choice of the spacelike hypersurface. Physically, this reflects the fact that the TAGPS-r is defined only in terms of the behavior of transversely emitted photons from σ_0 . For this reason, similarly to the DTTS, the definition of the TAGPS-r needs not be restricted to the setup of Subsec. 2.5.2. In particular, the TAGPS-r has the coordinate invariance in the following sense: If σ_0 is obtained as the TAGPS-r in the spacelike hypersurface Σ , on a different spacelike hypersurface Σ' which crosses Σ exactly at σ_0 , we can obtain σ_0 as the TAGPS-r as well.

For the TAGPS-r, Lemma 3.3 gives us the following theorem.

Theorem 3.21 ([15]). *We assume that M satisfies the Einstein equation (2.2) and Σ is an asymptotically flat spacelike maximal hypersurface equipped with the inverse mean curvature flow $\{\sigma_y\}_{y \in \mathbb{R}}$ where σ_0 is an TAGPS- r with $k \geq 0$. We suppose that each leaf σ_y is homeomorphic to a two-surface. If $\rho := T_{ab}n^a n^b \geq 0$ holds where n^a is the future-directed unit normal vector to Σ , the following inequality for the TAGPS- r σ_0 holds*

$$\begin{aligned} m_{\text{ADM}} + p_r^{(\text{int})} - m_{\text{ext}} &\geq \frac{\gamma_T}{3} \mathcal{R}_{A0} + \frac{\bar{J}_0^2 + \bar{J}_{\min}^2}{\mathcal{R}_{A0}^3} \\ &\geq \frac{\gamma_T}{3} \mathcal{R}_{A0} + 2 \frac{\bar{J}_{\min}^2}{\mathcal{R}_{A0}^3}. \end{aligned} \quad (3.107)$$

Proof. Considering the surface integral of Eq. (3.8) over σ_0 , and then, imposing the condition of Eq. (3.106), we have

$$\int_{\sigma_0} \left[\left(\gamma_T - \frac{3}{2} \right) {}^{(2)}R - G_{ab} r^a r^b - k \bar{K}_{(n)} + \frac{1}{2} (k^2 - k_{ab} k^{ab} - \tilde{\kappa}_{ab} \tilde{\kappa}^{ab}) + v_a v^a \right] dA \leq 0. \quad (3.108)$$

In the above, we used the fact that the time lapse function N is constant⁴ on σ_0 . Note that on σ_0 , κ_{ab} is a traceless quantity because of the condition of Eq. (3.104), i.e., $\kappa_{ab} = \tilde{\kappa}_{ab}$. Proposition 3.16 implies that the condition of Eq. (3.105) is rewritten as

$$-\bar{K}_{(n)} \geq \frac{1}{2} k, \quad (3.109)$$

so that with $k \geq 0$ on σ_0 ,

$$-\int_{\sigma_0} k \bar{K}_{(n)} dA \geq \frac{1}{2} \int_{\sigma_0} k^2 dA \quad (3.110)$$

holds. Thus, Eq. (3.108) with Eq. (3.110) implies

$$\int_{\sigma_0} k^2 dA \leq \frac{16\pi}{3} (3 - 2\gamma_T) + \frac{2}{3} \int_{\sigma_0} (16\pi P_r^{(\text{tot})} - 2v_a v^a) dA, \quad (3.111)$$

where we used the assumptions that the Einstein equation $G_{ab} = 8\pi T_{ab}$ holds for the spacetime (M, g_{ab}) and σ_0 is topologically sphere $\sigma_0 \approx S^2$. Then, Eqs. (3.13), (3.21) and (3.111) give us Eq. (3.107). \square

Note that in Eq. (3.111), if $P_r^{(\text{tot})} \leq 0$ is assumed on σ_0 ,

$$k = P_r^{(\text{tot})} = v_a = 0 \quad (3.112)$$

holds for $\gamma_T = 3/2$.

For vacuum and axisymmetric spacetimes, Eqs. (3.13), (3.24) and (3.111) give us the following theorem. The same arguments as those found in the LAGPS- r in Subsec. 3.2.2 can be made.

Theorem 3.22 ([15]). *Let M be a vacuum and axisymmetric spacetime satisfying the Einstein equation (2.2), and Σ be an asymptotically flat axisymmetric spacelike maximal hypersurface equipped with the inverse mean curvature flow $\{\sigma_y\}_{y \in \mathbb{R}}$ where σ_0 is an TAGPS- r with $k \geq 0$. We suppose that each leaf σ_y is homeomorphic to a two-surface. Then, we have an inequality for the TAGPS- r σ_0 ,*

$$m_{\text{ADM}} + p_{\text{gw}}^{(\text{int})} - m_{\text{gw}}^{(\text{ext})} \geq \frac{\gamma_T}{3} \mathcal{R}_{A0} + \frac{1 + \chi_0}{\mathcal{R}_0^2 \mathcal{R}_{A0}} J^2. \quad (3.113)$$

⁴As with the case of Eq. (3.94), Eq. (3.108) can be obtained even if N is not constant. Therefore, Theorems 3.21 and 3.22 hold even for non-constant N .

Chapter 4

Summary and outlook

As observable indicators of strong gravity regions, we reviewed the loosely trapped surface (LTS) and dynamically transversely trapping surface (DTTS) as an alternative to trapped surfaces. Additionally, we introduced the attractive gravity probe surface (AGPS) to characterize weak gravity region too, extending the LTS. We also presented the areal inequalities for these surfaces under certain conditions.

However, these inequalities did not account for contributions from angular momentum, gravitational waves, and matters. There was no extension of DTTS to encompass weak gravity regions. We reevaluated the AGPS proposed in Ref. [8] and subsequently introduced four types of AGPSs, including the original: the longitudinal AGPS associated with mean curvature (LAGPS-k) and Ricci scalar (LAGPS-r), and the transverse AGPS associated with mean curvature (TAGPS-k) and Ricci scalar (TAGPS-r). For these AGPSs, we proved the Penrose-like inequalities under certain conditions, taking account of the contributions from angular momentum, gravitational waves, and matters.

Our theorems require the assumption that spacelike hypersurface is maximal. However, for the Penrose inequality, there are attempts to relax such constraints [32]. Applying a similar analysis to our cases would be interesting. Comparing our results with those for stable isoperimetric surfaces [33] is also of interest.

Appendix A

Some geometric identities

We derive identities (3.4) and (3.9) used in the proofs of Proposition 3.1 and 3.2, respectively. We follow the same setup of Subsec. 2.5.2.

For the spacelike normal vector r^a of σ_0 on the spacelike hypersurface Σ , the derivative of r^a is calculated by

$$D_a r_b = (h_a^c + r_a r^c) D_c r_b, \quad (\text{A.1})$$

where D_a is the covariant derivative on Σ , and we used the induced metric of σ_0 , h_{ab} . The lapse function φ with respect to r^a gives us

$$(h_a^c + r_a r^c) D_c r_b = k_{ab} + r_a r^c D_c (\varphi D_b \varphi) \quad (\text{A.2})$$

$$= k_{ab} + r_a r^c r_b D_c \log \varphi + r_a r^c \varphi D_b (\varphi^{-1} r_c), \quad (\text{A.3})$$

where k_{ab} is the extrinsic curvature of σ_0 . Then, after some calculation, we have

$$D_a r_b = k_{ab} - r_a \mathcal{D}_b \log \varphi, \quad (\text{A.4})$$

where \mathcal{D}_a is the covariant derivative of σ_0 . The (r, r) -component of the Ricci tensor ${}^{(3)}R_{ab}$ on Σ is given by

$${}^{(3)}R_{ab} r^a r^b = {}^{(3)}R^c{}_{acb} r^a r^b \quad (\text{A.5})$$

$$= r^a (D^c D_a - D_a D^c) r_c \quad (\text{A.6})$$

$$= D^c (r^a D_a r_c) - D^c r^a D_a r_c - r^a D_a k, \quad (\text{A.7})$$

where k is the trace of k_{ab} . Thus, using Eq. (A.4), we obtain

$${}^{(3)}R_{ab} r^a r^b = -\varphi^{-1} \mathcal{D}^2 \varphi - k_{ab} k^{ab} - r^a D_a k. \quad (\text{A.8})$$

For the timelike normal vector n^a of σ_0 on the timelike hypersurface S , we also have

$$\bar{D}_a n_b = \kappa_{ab} + n_a \mathcal{D}_b \log N, \quad (\text{A.9})$$

where $\kappa_{ab} := h_a^c h_b^d K_{cd}$, N is the lapse function with respect to n^a and \bar{D}_a is the covariant derivative on S . Similar calculation of Eq. (A.8), by using the Ricci tensor ${}^{(3)}\bar{R}_{ab}$ on S , we obtain

$${}^{(3)}\bar{R}_{ab} n^a n^b = N^{-1} \mathcal{D}^2 N - \kappa_{ab} \kappa^{ab} - n^a \bar{D}_a \kappa. \quad (\text{A.10})$$

Bibliography

- [1] R. Penrose, Phys. Rev. Lett. **14**, 57-59 (1965).
- [2] S. W. Hawking and G. F. R. Ellis, *The large scale structure of space-time*, (Cambridge University Press, 1973).
- [3] R. M. Wald, *General Relativity*, (Chicago University Press, 1984).
- [4] S. W. Hawking, Commun. Math. Phys. **25**, 152-166 (1972).
- [5] C. M. Claudel, K. S. Virbhadra and G. F. R. Ellis, J. Math. Phys. **42**, 818-838 (2001).
- [6] T. Shiromizu, Y. Tomikawa, K. Izumi and H. Yoshino, PTEP **2017**, no.3, 033E01 (2017).
- [7] H. Yoshino, K. Izumi, T. Shiromizu and Y. Tomikawa, PTEP **2020**, no.2, 023E02 (2020).
- [8] K. Izumi, Y. Tomikawa, T. Shiromizu and H. Yoshino, PTEP **2021**, no.8, 083E02 (2021).
- [9] R. Penrose, Annals N. Y. Acad. Sci. **224**, 125-134 (1973).
- [10] P. S. Jang and R. M. Wald, J. Math. Phys. **18**, 41 (1977).
- [11] G. Huisken and T. Ilmanen, J. Diff. Geom. **59**, 353 (2001).
- [12] H. Bray, J. Diff. Geom. **59**, 177 (2001).
- [13] P. Anglada, Class. Quant. Grav. **35**, no.4, 045018 (2018).
- [14] K. Lee, T. Shiromizu and K. Izumi, Phys. Rev. D **105**, no.4, 044037 (2022).
- [15] K. Lee, T. Shiromizu, K. Izumi, H. Yoshino and Y. Tomikawa, Phys. Rev. D **106**, no.6, 064028 (2022).
- [16] A. Komar, Phys. Rev. **113**, 934-936 (1959).
- [17] K. Schwarzschild, Sitzungsber. Preuss. Akad. Wiss. Berlin (Math. Phys.) **1916**, 189-196 (1916).
- [18] M. D. Kruskal, Phys. Rev. **119**, 1743-1745 (1960).
- [19] R. P. Kerr, Phys. Rev. Lett. **11**, 237-238 (1963).
- [20] G. D. Birkhoff, *Relativity and Modern Physics*, (Harvard University Press, 1923).
- [21] G. L. Bunting and A. K. M. Masood-ul-Alam. Gen. Rel. Grav. **19**, 147-154 (1987).
- [22] P. T. Chrusciel, J. Lopes Costa and M. Heusler, Living Rev. Rel. **15**, 7 (2012);
M. Heusler, "Black hole uniqueness theorems," Cambridge University Press (1996).

- [23] R. H. Boyer and R. W. Lindquist, *J. Math. Phys.* **8**, 265 (1967).
- [24] R. Geroch, *Ann. N. Y. Acad. Sci.* **224**, 108 (1973).
- [25] R. L. Arnowitt, S. Deser and C. W. Misner, *Gen. Rel. Grav.* **40**, 1997-2027 (2008).
- [26] P. Anglada, M. E. Gabach-Clement and O. E. Ortiz, *Class. Quant. Grav.* **34**, no.12, 125011 (2017).
- [27] S. Dain, *Phys. Rev. Lett.* **112**, 041101 (2014).
- [28] M. A. Khuri, *J. Math. Phys.* **56**, no.11, 112503 (2015).
- [29] M. Reiris, *Gen. Rel. Grav.* **46**, 1777 (2014).
- [30] S. Dain, *Phys. Rev. Lett.* **96**, 101101 (2006).
- [31] S. Dain, *J. Diff. Geom.* **79**, no.1, 33-67 (2008).
- [32] E. Malec, M. Mars and W. Simon, *Phys. Rev. Lett.* **88**, 121102 (2002).
- [33] A. E. Acena and S. Dain, *Class. Quant. Grav.* **30**, 045013 (2013).